Inverse Analysis of Viscoelastic Stresses in Embryo Development

EEBE

Universitat Politècnica de Catalunya

January 23, 2019

Project Work

Sindre Korneliussen

Foreword

This project was written during the time-period from September 2018 until January 2019 under the supervision of Professor Jose J. Muñoz, UPC Dept. Mathematics.

The project analyses the set of plausible stresses that generate the observed deformations of central nervous system in Drosophila during the condensation process.

I want to thank my supervisor, Jose, of being great help during the development of this project, and Timothy Saunders' Lab at National University of Singapore (NUS) for the experimental data used in the analysis.

Contents

List of Figures

Abstract

From a set of planar displacements fields measured at different instants, stress profiles on 3D geometries have been created, modelled with finite elements. In the inverse analysis we are given a set of displacements and will rather consider the inverse problem. Using an inverse analysis, and velocity fields from a embryo development of a D. Melangostar a set of plausible stresses that generate the observed deformations of central nervous system in Drosophila during the condensation process have been analysed. This is with the use of different rheological models. From the post-processing of the Maxwell model there are characteristic behavior appearing.

There is an obvious oscillatory characteristic behavior in the embryo development. We are able to how the peak values of both stresses and strains in the larva during development is alternating between maximum and minimum values throughout the whole process, however with a tendency of decay. In addition it is shown how the larva seems to be consisting of different parts or segments along the AP-axis. We can from the oscillations through time see how the parts can be tracked along the displacement, but with a clear velocity in contracting direction. Initially in the beginning of deformation, a pattern alternating between compression and tension is obvious, once again highlighting the pattern of segmentation. The position of tension and compression can be tracked along time by studying the colormaps over time. An initial contraction phase is evident, while there is a trend of a decay or a pause phase, before finally there is a new contraction phase.

Abbreviations

AP-axis	Anterior Posterir axis
CNS	Central Nervous System
DOF	Degree of Freedom
FEM	Finite Element Method
Velo1(,3,4,5)	Velocity field 1(,3,4,5)

1 Introduction

1.1 Motivation

Drosophila Melangostar is today being used as a genetic model for several human diseases such as the neurodegenerative disorders Parkinson's, Huntington's, spinocerebellar ataxia and Alzheimer's disease. The fly is also being used to study mechanisms underlying aging and oxidative stress, immunity, diabetes, and cancer, as well as drug abuse.

Drosophila Melanogaster was among the first organisms used for genetic analysis, and today it is one of the most widely used and genetically best-known of all eukaryotic organisms. All organisms use common genetic systems; therefore, comprehending processes such as transcription and replication in fruit flies helps in understanding these processes in other eukaryotes, including humans.

The most used numerical technique within structural engineering is by far the finite element method (FEM), which is a method for numerical solution of field problems. A field problem is normally described by differential equations and associated boundary conditions, and the FEM provides an approximate solution to the mathematical problem. In the FEM, the mathematical model representing the real structure is discretized into a mesh of finite elements. This mesh is then represented by a system of algebraic equations to be solved for unknowns at the nodes, where the nodal unknowns are values of the field quantity, for instance displacements. In the inverse analysis we are given a set of displacements and will rather consider the inverse problem.

1.2 Background

Drosophila is today being used as a genetic model for several human diseases such as the neurodegenerative disorders Parkinson's, Huntington's, spinocerebellar ataxia and Alzheimer's disease. The fly is also being used to study mechanisms underlying aging and oxidative stress, immunity, diabetes, and cancer, as well as drug abuse.

There is a tremendous potential in the use of model genetic organisms such as the fruit fly, Drosophila Melanogaster. The similarity between mode of drug action, behavior, and gene response in Drosophila Melanogaster and mammalian systems, combined with the power of

genetics, have recently made the fly a very attractive system to study fundamental neuropharmacological processes relevant to human diseases.

There can be found several similarities between the Drosophila Melanogaster and humans. In 2000 there was a study comparing the fruit fly and human genome, done by National Human Genome Research Institute. The results showed some interesting numbers, about 60% of genes are conserved between the two species, about 75% of known human disease genes have a recognizable match in the genome of fruit flies and 50% of fly protein sequences have mammalian homologs.

A fly larvae can perform a large set of actions such as retraction, rolling or turning of parts. These movements are produced by a brain consisting of around 15,000 neurons(while an adult fruit fly contain approximately 135,000 neurons). In comparison a human brain have around 86 billions.

The Drosophila consists of an amount of neurons that makes mapping feasible, in addition to being complex enough to show interesting behaviours.

Other reasons that makes the fruit fly such a good model organism are:

- It requires little space, equipment reducing expenses compared to many other model organisms
- The Drosophila Melanogaster
- The fly has about only 10 days generation time, allowing the study of several generations in just weeks
- Females can lay up to 100 eggs a day, up to 2000 in a lifetime
- It is simply anesthetized
- Males and females are easily distinguished and isolated
- The mature larva has giant chromosomes in the salivary glands called polytene chromosomes, "puffs", which indicate regions of transcription, hence gene activity
- It has only four pairs of chromosomes - three autosomes, and one pair of sex chromosomes

These are just some of many pros of using the Drosophila Melanogaster.

In the search for new medical therapies, and in particular treatments for disorders of the central nervous system, there has been increasing recognition that identification of a single biological target is unlikely to be a recipe for success; a broad perspective is required. Understanding the complex interactions between the components within a given biological system that lead to modifications in output, such as changes in behavior or development, may be important avenues of discovery to identify new therapies.

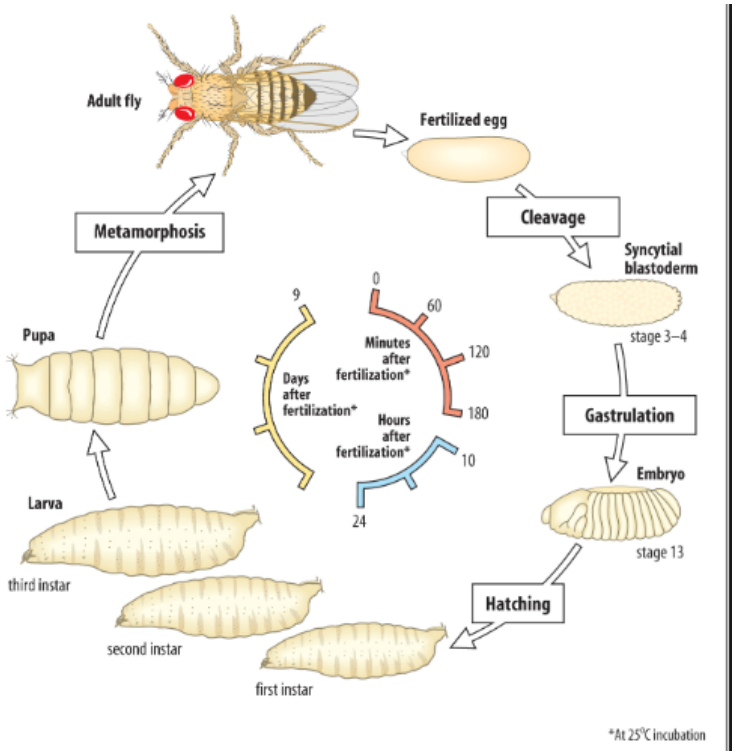

Figure 1.1: Drosophila life cycle

The reproductive life cycle of Drosophila at 25°C is approximately 10–12 days. An egg takes around 24 hours to undergo embryogenesis and hatch as a first instar larva. Just during the next 24 hours it will molt into a second instar larva, and another 24 hours the final and third instar larva stage is reached. The larva crawls out of the food substate and develops into an immobile pupa after 2 days in the third instar. The adult form transformation will take about 5-7 days, here a large physical change is done. The adult female is able to mate about 12 hours after eclosion. Importantly, a single female fly can lay hundreds of eggs within a few days. This short generation time and large number of progeny make it relatively easy to score thousands of mutants in a genetic screen in a matter of weeks.

The fly is a very different animal than a human. It seems somewhat amazing, therefore, that the molecular processes that generate a fly are quite similar to those that produce a person.

1.3 Objective

From a set of planar displacements fields measured at different instants, we can compute stress profiles on 3D geometries, modelled with finitie elements. A customised Matlab code will be employed and adapted to the problem at hand.

The report analyses the set of plausible stresses that generate the observed deformations of central nervous system in Drosophila during the condensation process.

Different rheological hypothesis will be tested, viscoelastic models of Maxwell and Kelvin types. From the analysis and post-process of results, suitable material parameters and models will be proposed for the embryonic tissue.

2 Theory

2.1 Elasticity

If a deformed material entirely recovers the original shape when the acting forces causing the deformation is removed, and if the material under isothermal conditions, experience a one-one relation between stress and strain, we consider the material as elastic.

We have the elastic stress-strain relation:

$$\sigma = \sigma(\varepsilon) \tag{1}$$

Or the inverse relation:

$$\varepsilon = \varepsilon(\sigma) \tag{2}$$

2.1.1 Some characteristics

- Reversible
  The body return to the original shape after unloading
- Path independence
  There is a one-to-one relation of stress and strain
- No energy dissipation
  An elastic element such as the spring will not dissipate energy.
- Rate independence
  Rate of loading will not affect the response of the model

If the material is considered to be linear elastic the stress-strain relationship can be written as follows:

$$\sigma = E\varepsilon \tag{3}$$

Which simplifies the general strain energy function:

$$U_0(\varepsilon) = \int_0^{\varepsilon} \sigma(\varepsilon) d\varepsilon \tag{4}$$

To the following function which yields for linear elasticity:

$$U_0(\varepsilon) = \frac{1}{2}E\varepsilon^2 \tag{5}$$

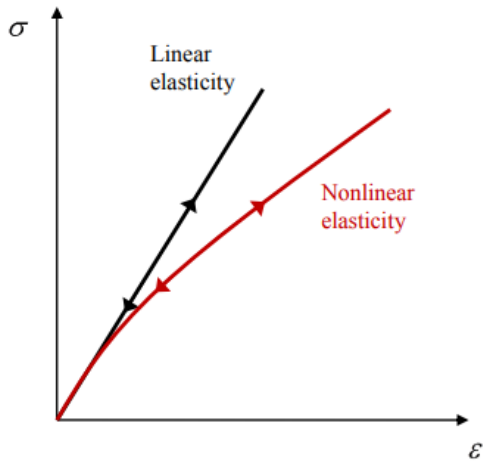

Figure 2.1: Linear and nonlinear behaviour

Notice that for an elastic material, the path for loading and unloading will be the same.

2.1.2 Linearity

The material is said to be linear elastic if the relation between the state of stress and state of strain is linear. The generalized Hooke's law defines the most general form of a linear elastic material.

$$\sigma_{ij} = C_{ijkl}\varepsilon_{kl} \tag{6}$$

$$\sigma_{ij} = \begin{bmatrix} \sigma_{11} \\ \sigma_{22} \\ \sigma_{33} \\ \sigma_{23} \\ \sigma_{31} \\ \sigma_{12} \end{bmatrix}$$

$$C = \begin{bmatrix} C_{1111} & C_{1122} & C_{1133} & C_{1123} & C_{1131} & C_{1112} \\ C_{2211} & C_{2222} & C_{2233} & C_{2223} & C_{2231} & C_{2212} \\ C_{3311} & C_{3322} & C_{3333} & C_{3323} & C_{3331} & C_{3312} \\ C_{2311} & C_{2322} & C_{2333} & C_{2323} & C_{2331} & C_{2312} \\ C_{3111} & C_{3122} & C_{3133} & C_{3123} & C_{3131} & C_{3112} \\ C_{1211} & C_{1222} & C_{1233} & C_{1223} & C_{1231} & C_{1212} \end{bmatrix}$$

$$\varepsilon_{ij} = \begin{bmatrix} \varepsilon_{11} \\ \varepsilon_{22} \\ \varepsilon_{33} \\ \gamma_{23} \\ \gamma_{31} \\ \gamma_{12} \end{bmatrix}$$

Where the C is consisting of the Lame constants λ and ν

It is also noted that the matrix consisting of 81 components is reduced drastically due to the symmetry of the stress and strain tensors, there are only 6 independent constitutive equations for the linear elastic material. The number of independent coefficients is then reduced to 36 due the minor symmetries. In linearity we can reduce the number of parameters in the C matrix to 21 for a fully anisotropic material, nine for orthotropic materials and only two if the material is isotropic.

2.1.3 Isotropy

If the behaviour of the material is independent of the orientation, we call it an isotropic material.

With the lamé constants we may express C

$$C_{ijkl} = \lambda\delta_{ij}\delta_{kl} + \mu(\delta_{ik}\delta_{jl} + \delta_{il}\delta_{jk}) \tag{7}$$

Furthermore we can express the stresses

$$\sigma_{ij} = C_{ijkl}\varepsilon_{kl} = \lambda\varepsilon_{kk}\delta_{ij} + 2\mu\varepsilon_{ij} \tag{8}$$

Linear isotropic elasticity equations
(1) Equilibium equations
(2) Kinematic relations
(3) Constitutive equations

Lamé equations

$$\lambda = \frac{E\nu}{(1+\nu)(1-2\nu)} \tag{9}$$

$$\mu = \frac{E}{2(1+\nu)} \tag{10}$$

$$\begin{aligned} \varepsilon_{xx} &= \frac{1}{E}\left[\sigma_{xx} - \nu(\sigma_{yy} + \sigma_{zz})\right] \quad \varepsilon_{xy} = \tfrac{1}{2G}\sigma_{xy} \\ \varepsilon_{yy} &= \frac{1}{E}\left[\sigma_{yy} - \nu(\sigma_{xx} + \sigma_{zz})\right] \quad \varepsilon_{xz} = \tfrac{1}{2G}\sigma_{xz} \\ \varepsilon_{zz} &= \frac{1}{E}\left[\sigma_{zz} - \nu(\sigma_{xx} + \sigma_{yy})\right] \quad \varepsilon_{yz} = \tfrac{1}{2G}\sigma_{yz} \end{aligned}$$

Figure 2.2: Strains in three dimensions

2.2 Viscoelasticity

The material exhibits both viscous(fluid-like) and elastic(solid-like) characteristics, it has time-dependent elastic properties. It is common to describe the viscoelastic materials using rheological models composed of springs and dashpots.

2.2.1 Some characteristics

- Reversible/irreversible
  The body may return to the original shape after unloading
- Path dependence
  There is not necessarily a one-to-one relation of stress and strain

- Energy dissipation
  While an elastic element such as the spring will not dissipate energy, the inelastic dashpot contributes to a dissipation
- Rate dependence
  Rate of loading will affect the response of the model

2.2.2 Maxwell model

This model is composed by a spring and a dashpot connected in series. The spring contributes with the elastic displacement is ε^e, while the viscoelastic displacement ε^v is a contribution of the inelastic dashpot.

$$\varepsilon = \varepsilon^e + \varepsilon^v \tag{11}$$

Which again leads to the relation

$$\dot{\varepsilon} = \dot{\varepsilon^e} + \dot{\varepsilon^v} \tag{12}$$

With the total strain rate, $\dot{\varepsilon}$, being the sum of the elastic and viscoelastic strain rate.

The stress experienced or applied has to be equal for both elements as we consider them in series. This means that the total stress is equal to the stress in the spring, which again is equal to the stress in the dashpot.

$$\sigma = \sigma^e = \sigma^v \tag{13}$$

Equation (3) shows the relation between the elastic strain and stress, and is the stress contribution from the linear spring in a viscoelastic model. In viscoelasticity we include the stress produced by the inelastic dashpot. The following relation shows the behaviour of a viscous material with η being the viscosity constant

$$\sigma = \eta\dot{\varepsilon^v} \tag{14}$$

This equation also demonstrate how the rate dependency of a viscoelastic material is introduced.

If we consider the time derivative of equation (3) as the elastic strain we have

$$\dot{\varepsilon^e} = \frac{\dot{\sigma}}{E} \tag{15}$$

Equation (9), (10) and (11) gives the strain rate of the Maxwell model

$$\dot{\varepsilon} = \frac{\dot{\sigma}}{E} + \frac{\sigma}{\eta} \tag{16}$$

This differential equation can be solved, let's consider these cases:

- ε is constant and positive
  Having $\dot{\varepsilon} = 0$ and solving for the stress gives us $\sigma = \sigma_0 e^{-\frac{t}{\tau}}$
  Where $\sigma_0 = E\varepsilon_0$
  And $\tau = \frac{\eta}{E}$

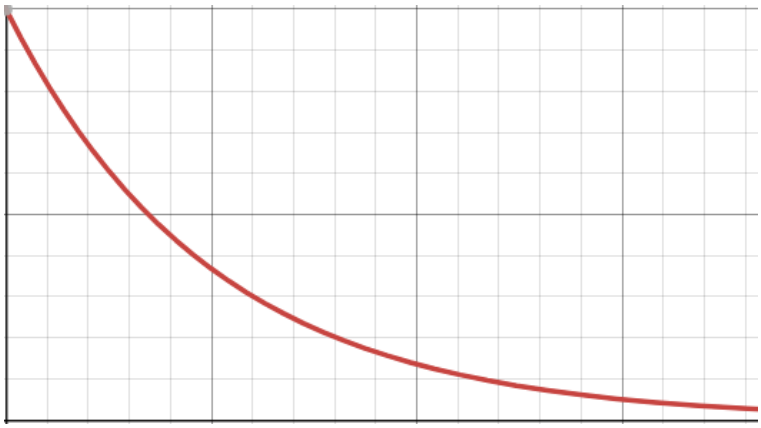

Figure 2.3: Maxwell non-incremental, arbitrary values

- $\dot{\varepsilon}$ is constant and positive
  The stres is now also a function of the strain rate $\sigma = \eta\dot{\varepsilon}(1 - e^{-\frac{t}{\tau}})$ and it will eventually reach the value of $\eta\dot{\varepsilon}$.

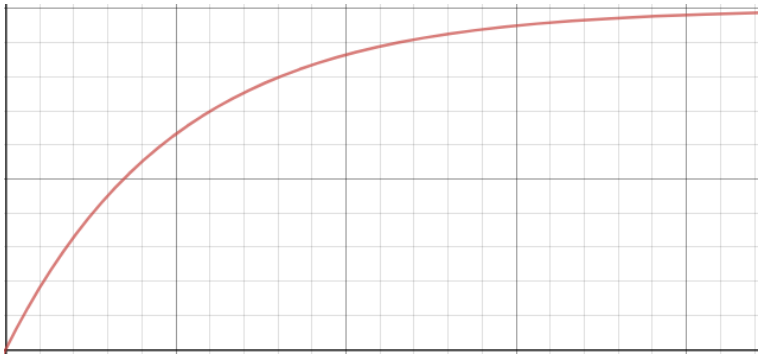

Figure 2.4: Maxwell incremental, arbitrary values

Note that the plots are for arbitrary values, only to represent the behavior. Different material values will alter the labels.

2.2.3 Kelvin-Voigt model

In common with the Maxwell model, the Kelvin-Voigt model describes viscoelastic behaviour with the use of rheological elements such as the spring and the dashpot. For the latter model we will consider the elements to be in parallel rather than in series.

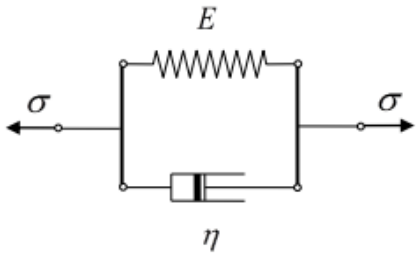

Figure 2.5: Kelvin-Voigt Model

In this model the strain and strain-rate are equal for both elements, however the stresses may now be different.

$$\varepsilon = \varepsilon^e = \varepsilon^v \tag{17}$$

Considering the equation (3) and (11) in addition to the relation $\sigma = \sigma^e + \sigma^v$ we have

$$\sigma = E\varepsilon^{e} + \eta\dot{\varepsilon^{v}} \tag{18}$$

This is also a solvable equation, let's consider these cases:

- ε is constant and positive
  Having $\dot{\varepsilon} = 0$ and solving for the stress gives us $\sigma = E\varepsilon$

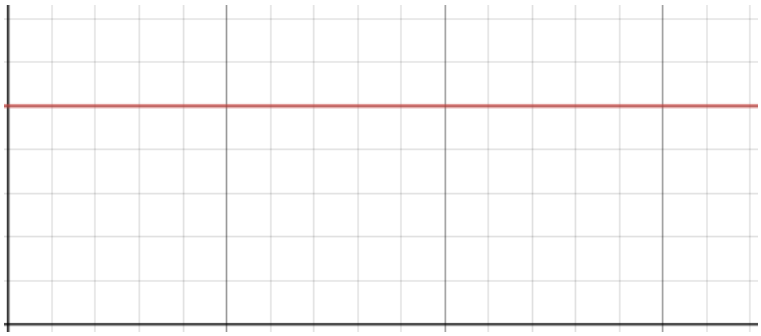

Figure 2.6: Kelvin non-incremental, arbitrary values

- $\dot{\varepsilon}$ is constant and positive
  The stress is now also a function of the strain rate $\sigma = E\varepsilon + \eta\dot{\varepsilon}$

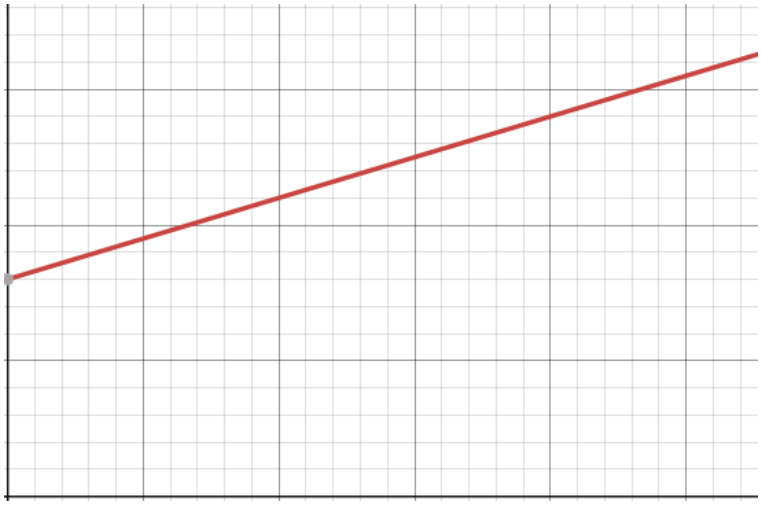

Figure 2.7: Kelvin incremental, arbitrary values

3 Deduction of Stress Evolution

The finite element (FE) method is a numerical method for solving boundary value problems (BVP), i.e., problems that can be formulated by a set of partial differential equations and associated boundary conditions. The method is formulated from the weak form of the BVP, which in our case is the principle of virtual work

3.1 Discretization

Displacements are interpolated within the elements

$$\mathbf{u}(x) = \mathbf{N_e}(\mathbf{x})\mathbf{v_e}(\mathbf{t}), \qquad \mathbf{x} \in V_e \tag{19}$$

Where we have the shape(or interpolation) functions $\mathbf{N}$ which is a matrix, displacement vector $\mathbf{u}$, the nodal displacement vector $\mathbf{v_e}$ and the position vector $\mathbf{x}$, $\mathbf{x} \in V$

Further we have the relation between the degrees of freedom of an element and the degrees of freedom of the structure $\mathbf{v_e}(t) = \mathbf{a_e}\mathbf{r}(t)$. Here $\mathbf{r}$ is the global nodal displacement vector. Through the connectivity matrix $\mathbf{a}_e$ we can obtain the global shape functions in addition to the global displacements. The global displacement $\mathbf{u}$ can be presented as follows

$$\mathbf{u}(x,t) = \sum_{e=1}^{n_e} \mathbf{N_e}(x)\mathbf{v_e}(t) = \sum_{e=1}^{n_e} \mathbf{N_e}(x)\mathbf{a_e}\mathbf{r} = \mathbf{N}(x)\mathbf{r}(t), \qquad \mathbf{x} \in V \tag{20}$$

With the global shape function

$$\mathbf{N}(x) = \sum_{e=1}^{n_e} \mathbf{N_e}(x)\mathbf{a_e}, \qquad \mathbf{x} \in V \tag{21}$$

$$\varepsilon(x,t) = \mathbf{\Delta}\mathbf{u}(x,t) = \mathbf{\Delta}\mathbf{N}(x)\mathbf{r}(t) = \mathbf{B}(x)\mathbf{r}(t) \tag{22}$$

Where $\mathbf{\Delta}$ is a differential operator

$$\mathbf{\Delta} = \begin{bmatrix} \frac{\partial}{\partial x_1} & 0 & 0 \\ 0 & \frac{\partial}{\partial x_2} & 0 \\ 0 & 0 & \frac{\partial}{\partial x_3} \\ 0 & \frac{\partial}{\partial x_3} & \frac{\partial}{\partial x_2} \\ \frac{\partial}{\partial x_3} & 0 & \frac{\partial}{\partial x_1} \\ \frac{\partial}{\partial x_2} & \frac{\partial}{\partial x_1} & 0 \end{bmatrix} \tag{23}$$

The resulting vector will be

$$\varepsilon = \begin{bmatrix} \varepsilon_{11} \\ \varepsilon_{22} \\ \varepsilon_{33} \\ \gamma_{23} \\ \gamma_{31} \\ \gamma_{12} \end{bmatrix}$$

Where $\gamma_{23} = 2\varepsilon_{23}$, $\gamma_{31} = 2\varepsilon_{31}$ and $\gamma_{12} = 2\varepsilon_{12}$

Now we can apply the principle of virtual work, virtual displacements are $\delta\mathbf{u}(x) = \mathbf{N}(x)\delta\mathbf{r}$ where $\mathbf{x} \in V$. This will give us the relation between virtual strains and virtual displacements.

$$\delta\varepsilon = \Delta\delta\mathbf{u} = \mathbf{B}\delta\mathbf{r}, \qquad \mathbf{x} \in V \tag{24}$$

The principle of virtual work is then expressed

$$\int_V \delta\varepsilon^T \sigma dV = \int_V \delta\mathbf{u}^T \mathbf{b} dV + \int_{S_i} \delta\mathbf{u}^T \mathbf{t} dS, \qquad \forall\delta\mathbf{u} \tag{25}$$

$\mathbf{b}$ being the body forces and $\mathbf{t}$ being the traction vectors. If we insert the interpolated displacement field we obtain the following

$$\delta\mathbf{r}^T [\int_V \mathbf{B}^T \sigma dV - \int_V \mathbf{N}^T \mathbf{b} dV - \int_{S_i} \mathbf{N}^T \mathbf{t} dS] = 0, \qquad \forall\delta\mathbf{r} \tag{26}$$

Which implies that

$$\int_V \mathbf{B}^T \sigma dV + \int_V \mathbf{N}^T \mathbf{b} dV + \int_{S_i} \mathbf{N}^T \mathbf{t} dS = 0 \tag{27}$$

From this equation it is now useful to consider the internal and external nodal forces.

$$\mathbf{R}^{int} = \int_V \mathbf{B}^T \sigma dV \tag{28}$$

$$\mathbf{R}^{ext} = \int_V \mathbf{N}^T \mathbf{b} dV + \int_{S_i} N^T \mathbf{t} dS \tag{29}$$

$$\mathbf{R}^{int} = \mathbf{R}^{ext} \tag{30}$$

3.2 Linear Elastic

In the case of linear elasticity we have the constitutive relation

$$\sigma = \mathbf{C}\varepsilon \tag{31}$$

$$\mathbf{C} = \frac{E}{(1-2\nu)(1+\nu)} \begin{bmatrix} 1-\nu & \nu & \nu & 0 & 0 & 0 \\ \nu & 1-\nu & \nu & 0 & 0 & 0 \\ \nu & \nu & 1-\nu & 0 & 0 & 0 \\ 0 & 0 & 0 & \frac{1-2\nu}{2} & 0 & 0 \\ 0 & 0 & 0 & 0 & \frac{1-2\nu}{2} & 0 \\ 0 & 0 & 0 & 0 & 0 & \frac{1-2\nu}{2} \end{bmatrix} \tag{32}$$

Combining Hooke's law for a linear elastic material with equation (22) we obtain

$$\sigma = \mathbf{CBr} \tag{33}$$

Meaning that the internal force vector from equation (28) will be

$$\mathbf{R}^{int} = \int_V \mathbf{B}^T \mathbf{CBr} dV \tag{34}$$

$$\mathbf{R}^{int} = \mathbf{r} \int_V \mathbf{B}^T \mathbf{CB} dV \tag{35}$$

Where $\mathbf{K}$ is given as

$$\mathbf{K} = \int_V \mathbf{B}^T \mathbf{C} \mathbf{B} dV \tag{36}$$

We therefore have

$$\mathbf{R}^{int} = \mathbf{K}\mathbf{r} \tag{37}$$

Which also implies the more known relation from linear finite element method

$$\mathbf{K}\mathbf{r} = \mathbf{R}^{ext} \tag{38}$$

3.3 Maxwell Model

$$\varepsilon = \varepsilon^e + \varepsilon^v \tag{39}$$

$$\sigma^e = D\varepsilon^e \tag{40}$$

$$\sigma^v = \eta \dot{\varepsilon^v} \tag{41}$$

Since $\sigma = \sigma^e = \sigma^v$, we have the following.

$$D\varepsilon^e = \eta \dot{\varepsilon^v} \tag{42}$$

By evaluating the next strain in time-steps we can use that $\varepsilon_{n+1} = \varepsilon_n + \Delta\varepsilon_{n+1}$. This will further make equation (41)

$$D\varepsilon^e_{n+\theta} = \eta \dot{\varepsilon^v} = \frac{\eta}{\Delta t}(\varepsilon^v_{n+1} - \varepsilon^v_n) = \frac{\eta}{\Delta t}[(\varepsilon_{n+1} - \varepsilon^e_{n+1}) - (\varepsilon_n - \varepsilon^e_n)] \tag{43}$$

Here the notation of $\varepsilon^e_{n+\theta}$ means that we have discretized ε such that $\varepsilon_{n+\theta} = (1-\theta)\varepsilon_n + \theta\varepsilon_{n+1}$, and $0 \leq \theta \leq 1$

$$\frac{\Delta t}{\eta} D(\theta\varepsilon^e_{n+1} + (1-\theta)\varepsilon^e_n) = \varepsilon_{n+1} - \varepsilon^e_{n+1} - \varepsilon_n + \varepsilon^e_n \tag{44}$$

With some simplifications we can obtain an expression for the next time-step of the elastic strain.

$$\varepsilon^e_{n+1} = (I + \theta\frac{\Delta t}{\eta}D)^{-1}[\varepsilon_{n+1} - \varepsilon_n + \varepsilon^e_n(I - (1-\theta)\frac{\Delta t}{\eta}D)] \tag{45}$$

$$\mathbf{R}^{int} = \int_V \mathbf{B}^T \sigma dV \tag{46}$$

With $\sigma = D\varepsilon$

$$\mathbf{R}^{int} = \int_V \mathbf{B}^T \mathbf{D} \boldsymbol{\varepsilon}^{\mathbf{e}}_{\mathbf{n+1}} dV \tag{47}$$

$$\mathbf{R}^{int} = \int_V \mathbf{B}^T \mathbf{D}(I + \theta\frac{\Delta t}{\eta}D)^{-1}[\varepsilon_{n+1} - \varepsilon_n + \varepsilon^e_n(I - (1-\theta)\frac{\Delta t}{\eta}D)]dV \tag{48}$$

$$\mathbf{R}^{int} = \int_V \mathbf{B}^T \mathbf{D}^* \varepsilon_{n+1} - \int_V \mathbf{B}^T \mathbf{D}^* \varepsilon_n + \int_V \mathbf{B}^T \mathbf{D}^* \varepsilon^e_n (I - (1-\theta)\frac{\Delta t}{\eta}\mathbf{D}) \tag{49}$$

Where we have used that

$$D^* = D(I + \frac{\Delta t}{\eta}\theta D)^{-1} \tag{50}$$

Further we have

$$\mathbf{R}^{int} = \int_V \mathbf{B}^T \mathbf{D}^* \varepsilon_{n+1} - \int_V \mathbf{B}^T \mathbf{D}^* \varepsilon_n + \int_V \mathbf{B}^T \mathbf{D}^* (\mathbf{D}^{-1} - (1-\theta)\frac{\Delta t}{\eta})\varepsilon^e_n \mathbf{D} \tag{51}$$

$$\mathbf{R}^{int} = \int_V \mathbf{B}^T \mathbf{D}^* \varepsilon_{n+1} - \int_V \mathbf{B}^T \mathbf{D}^* \varepsilon_n + \int_V \mathbf{B}^T \mathbf{D}^* (\mathbf{D}^{-1} - (1-\theta)\frac{\Delta t}{\eta})\sigma_n \tag{52}$$

$$\mathbf{R}^{int} = \int_V \mathbf{B}^T \mathbf{D}^* \varepsilon_{n+1} + \int_V \mathbf{B}^T \mathbf{D}^* ((\mathbf{D}^{-1} - (1-\theta)\frac{\Delta t}{\eta})\sigma_n) - \varepsilon_n) \tag{53}$$

Renaming equation (52) respectively

$$\mathbf{R}^{int} = \mathbf{K}^* \mathbf{r} - \mathbf{R}^{int}_n + \mathbf{R}^{\sigma}_n \tag{54}$$

3.4 Kelvin-Voigt

In this model the elements are in parallel, thus we have

$$\varepsilon = \varepsilon^e = \varepsilon^v \tag{55}$$

Stresses are then given as

$$\sigma = \sigma^e + \sigma^v = D\epsilon^e + \eta\dot{\varepsilon}^v \tag{56}$$

$$\sigma^e = D[\varepsilon_n(1-\theta) + \varepsilon_{n+1}\theta] \tag{57}$$

$$\sigma^v = \frac{\eta}{\Delta t}(\varepsilon_{n+1} - \varepsilon_n) \tag{58}$$

$$\mathbf{R}^{int} = \int_V \mathbf{B}^T \sigma dV \tag{59}$$

$$\mathbf{R}^{int} = \int_V \mathbf{B}^T (\sigma^e + \sigma^v) dV \tag{60}$$

$$\mathbf{R}^{int} = \int_V \mathbf{B}^T \sigma^e dV + \int_V \mathbf{B}^T \sigma^v dV \tag{61}$$

$$\mathbf{R}^{int} = \int_V \mathbf{B}^T D[\varepsilon_n(1-\theta) + \varepsilon_{n+1}\theta] dV + \int_V \mathbf{B}^T \frac{\eta}{\Delta t}(\varepsilon_{n+1} - \varepsilon_n) dV \tag{62}$$

$$\mathbf{R}^{int} = \theta \int_V \mathbf{B}^T \mathbf{D} \varepsilon_{n+1} dV + (1-\theta) \int_V \mathbf{B}^T \mathbf{D} \varepsilon_n dV + \frac{\eta}{\Delta t} \int_V \mathbf{B}^T \varepsilon_{n+1} - \frac{\eta}{\Delta t} \int_V \mathbf{B}^T \varepsilon_n \tag{63}$$

$$\mathbf{R}^{int} = \theta \int_V \mathbf{B}^T \mathbf{D} \varepsilon_{n+1} dV + (1-\theta) \int_V \mathbf{B}^T \mathbf{D} \varepsilon_n dV + \frac{\eta}{\Delta t} \int_V \mathbf{B}^T \varepsilon_{n+1} dV - \frac{\eta}{\Delta t} \int_V \mathbf{B}^T \varepsilon_n dV \tag{64}$$

Where we again may find the K matrices

$$\mathbf{K}^e = \theta \int_V \mathbf{B}^T \mathbf{D} \mathbf{B} dV \tag{65}$$

$$\mathbf{K}^v = \frac{\eta}{\Delta t} \int_V \mathbf{B}^T \mathbf{B} dV \tag{66}$$

Section 3.3 and 3.4 show how the problem is modelled in matlab.

4 Method and Validation

The script given at hand is solving a inverse problem, where we have the deformations but not the stresses. Initially the script was tested with geometries and deformations that can simply be calculated numerically and analytical.

4.1 GiD

The geometry we use to test the script is a 1x1x1 cube, created in GiD as shown below.

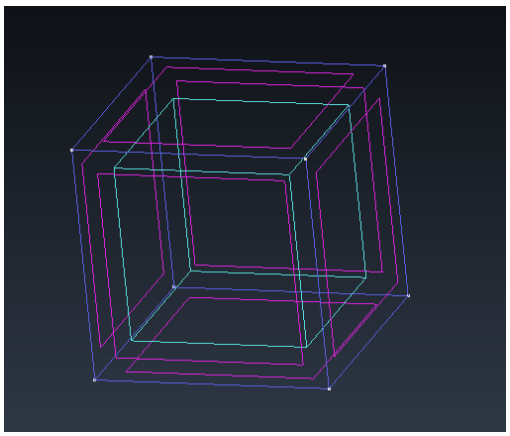

Figure 4.1: Test geometry

The initial mesh used is consisting of only one hexedral element.

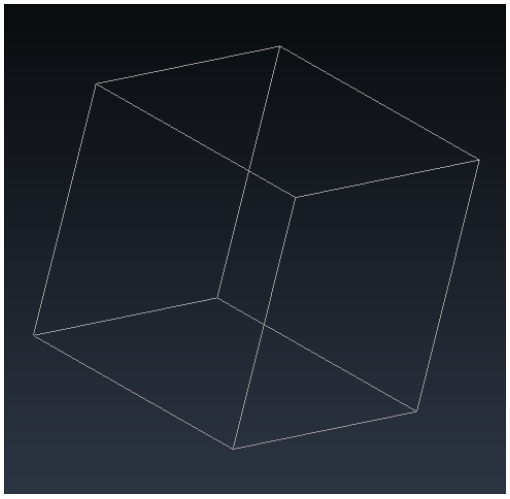

Figure 4.2: Test mesh

Further a code to generate displacements on the initial mesh of the cube was created

In order to obtain the values of only a single point in the cube, some modifications are done in the mainFEM code, which stores values of stresses and strains of a given point throughout the whole deformation process.

With the FEM script given I will consider the different models for different displacement histories, different material constants, and different meshes, then I will compare the results with the analytic one for each case. In addition to a analytical result, I have also numerically approximated the solution with the use of a finite difference method setting θ equal to 0.5. This way it can be spotted if there is reason to believe that numerical errors are generated in the main script.

4.2 Kelvin-Voigt Model

- E = 1000
- $\eta = 1000 - 10000$
- nt = 100
- displacement = 1
- $\varepsilon = \frac{displacement}{nt}$

From equation (18) we have $\sigma = E\varepsilon^e + \eta\dot{\varepsilon^v}$

We will first look at the non-incremental displacement case, which simplifies the equation to

$$\sigma_{Nk} = E\varepsilon_N \tag{67}$$

We consider just one element in the simulation.

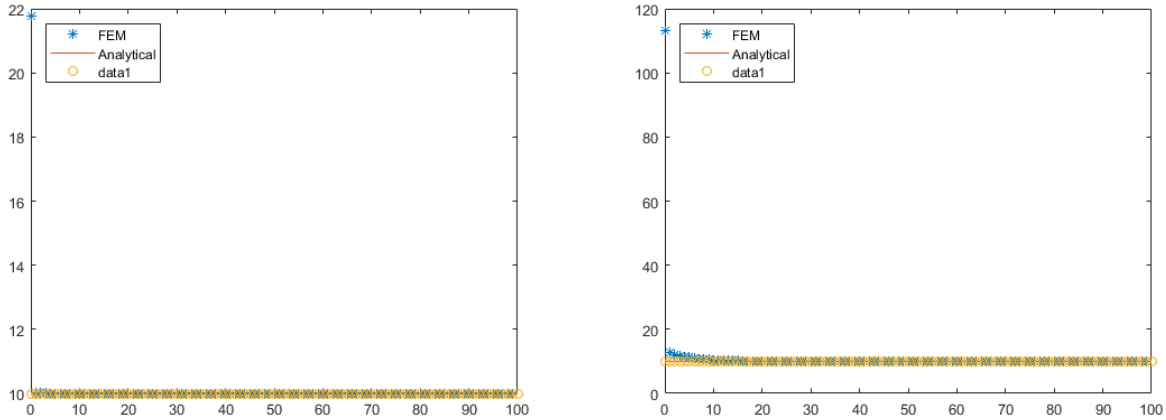

(a) $\eta = 1000$ **(b)** $\eta = 10000$

Figure 4.3: Kelvin-Voigt non incremental with 1 unit displacement

It finite difference method is given the name data1 for all plots.

Again, from equation (18), we obtain the incremental displacement case.

$$\sigma_k = E\varepsilon + \eta\dot{\varepsilon} \tag{68}$$

We will again look at the following scenario.

- E = 1000
- $\eta = 10000$
- nt = 100
- displacement = 1
- $\varepsilon = \frac{displacement}{nt}$

But this time we will consider an incremental displacement field.

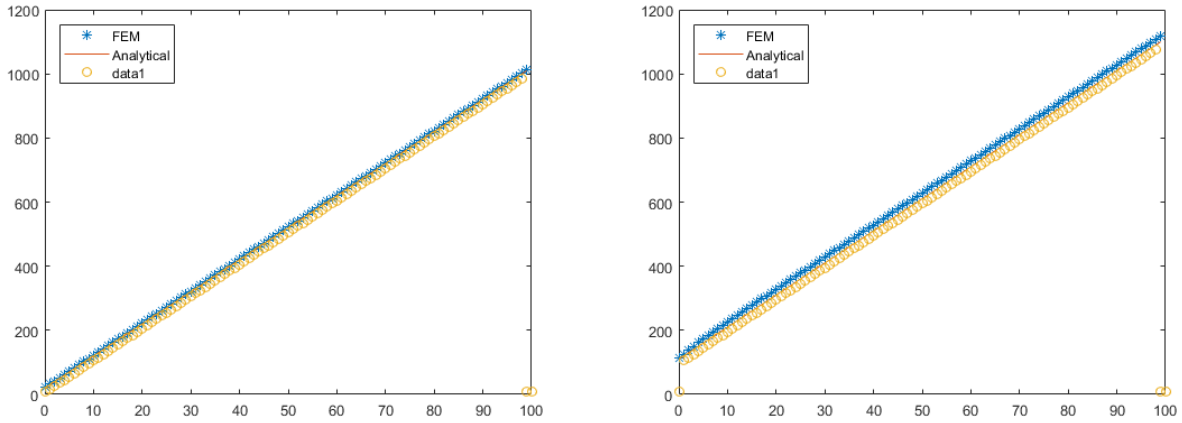

(a) $\eta = 1000$ **(b)** $\eta = 10000$

Figure 4.4: Kelvin-Voigt incremental with 1 unit displacement

4.3 Maxwell Model

- E = 1000
- $\eta = 10000$
- nt = 100
- displacement = 1
- $\varepsilon = \frac{displacement}{nt}$

If we look at the case where the strain is constant, we will have the strain rate equal to zero. Thus the Maxwell model can be written as follows.

$$\sigma_0 = E\varepsilon_0 \tag{69}$$

$$\sigma_{Nm} = \sigma_0 e^{-\frac{t}{\tau_c}} \tag{70}$$

Where $\tau_c = \frac{\eta}{E}$

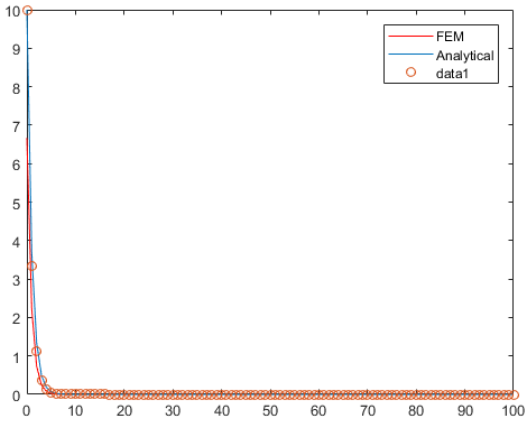

(a) $\eta = 1000$

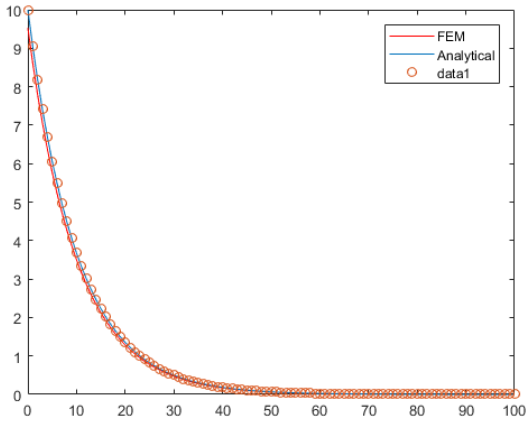

(b) $\eta = 10000$

Figure 4.5: Maxwell non-incremental with 1 unit displacement

Now running consecutively the same values with incremental displacement

The analytic equation have now changed

$$\sigma_m = \eta\dot{\varepsilon}(1 - e^{-\frac{t}{\tau_c}}) \tag{71}$$

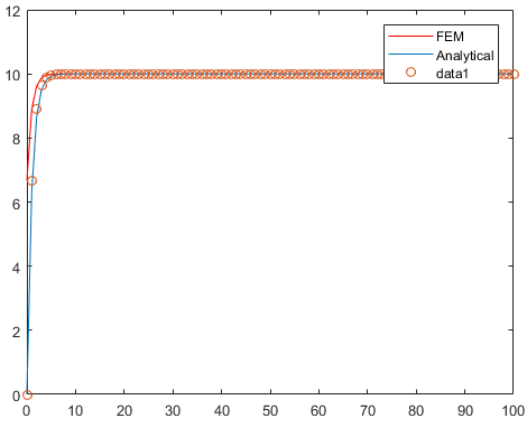

(a) $\eta = 1000$

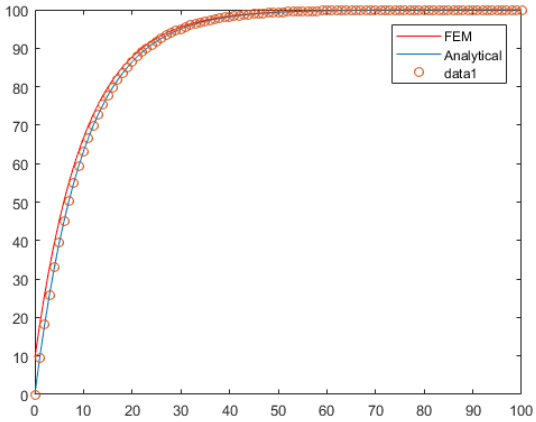

(b) $\eta = 10000$

Figure 4.6: Maxwell incremental with 1 unit displacement

All plots presented above show more or less coincident values between the three ways of

modelling the problem.

5 Results

Given is the geometry of Drosophila during the condensation process and the generated deformations that follow. From the geometry and displacement I will now present the varying stresses that are produced when different material parameters and different rheological material models are taken into account. The stresses are a result of a many factors that yet are to be set. Therefore the stresses presented will be a set of plausible stresses for all cases.

The data used is made by Sham L. Tlili at Timothy Saunders' Lab at National University of Singapore (NUS) with 2-photon microscopy. We are considering looking at geometry files of a curved CNS, in addition to a set of velocity fields.

5.1 Theory

5.1.1 Element and mesh

The element used in the data are hexahedra elements.

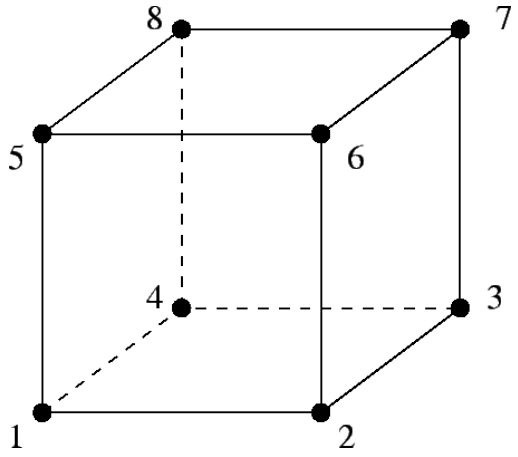

Figure 5.1: 8 noded hexahedron

The tri-linear hexahedron has eight nodes and is often called the eight-node brick element.

The eight-node brick element is analogous to the four-node plane Q4 element, and has the defect of shear locking.

The hexahedral element can be of arbitrary shape if it is formulated as an isoparametric element, with the six faces of the reference element defined by $\xi = \pm 1$, $\eta = \pm 1$, $\zeta = \pm 1$

The shape functions of the eight-node element are given by

$$\mathbf{N_i}(\xi, \eta, \zeta) = \frac{1}{8}(1 + \xi_i\xi)(1 + \eta_i\eta)(1 + \zeta_i\zeta) \tag{72}$$

5.1.2 Characteristic time

The characteristics of viscoelastic materials are most often determined from creep tests, stress relaxation tests and cyclic tests. The latter tests are used to characterize the hysteresis seen in the stress-strain curve, i.e., the energy loss (or dissipation) during each loading cycle.

Close temperature control of the fluid is essential to acquire accurate measurements, particularly in materials like lubricants, whose viscosity can double with a change of only 5 °C. For some fluids, the viscosity is constant over a wide range of shear rates (Newtonian fluids). The fluids without a constant viscosity (non-Newtonian fluids) cannot be described by a single number. Non-Newtonian fluids exhibit a variety of different correlations between shear stress and shear rate.

Characteristic time is given as

$$\tau = \frac{\eta}{E} \tag{73}$$

τ is measured in seconds(s).

To see how the characteristic time affects our viscoelastic models, let us quickly repeat the solution of the differential equations of the Maxwell model and the Kelvin model.

- ε is constant and positive
  Having $\dot{\varepsilon} = 0$ and solving for the stress gives us $\sigma = \sigma_0 e^{-\frac{t}{\tau}}$
  Where $\sigma_0 = E\varepsilon_0$
  And $\tau = \frac{\eta}{E}$

- $\dot{\varepsilon}$ is constant and positive
  The stres is now also a function of the strain rate $\sigma = \eta\dot{\varepsilon}(1 - e^{-\frac{t}{\tau}})$ and it will eventually reach the value of $\eta\dot{\varepsilon}$.

And for the Kelvin Model we have the following solutions

- ε is constant and positive
  Having $\dot{\varepsilon} = 0$ and solving for the stress gives us $\sigma = E\varepsilon$

- $\dot{\varepsilon}$ is constant and positive
  The stress is now also a function of the strain rate $\sigma = E\varepsilon + \eta\dot{\varepsilon}$

Here we may see how the relaxation time determines the stress curve. By changing the characteristic time as material parameters we should expect to obtain different results for these models. What we can expect is that a reduction of the characteristic time will also result in a reduction in stress.

Let us first have a look at the stresses generated in a 1x1x1 cube for the different models with varying characteristic time, using the inverse analysis code.

The cube is created in GiD and is equal to the one used for validation. Also the same code used to apply the displacement for the validation is used. Again, in order to obtain the values of only a single point in the cube, some modifications are done in the mainFEM code, which stores values of stresses and strains of a given point throughout the whole deformation.

Firstly let us consider a Kelvin-Voigt model, using the following parameters

- E = 1000
- η = 1000 & 10000
- nt = 100
- displacement = 1
- $\varepsilon = \frac{displacement}{nt}$
- dt=1
- $\theta = 0.5$

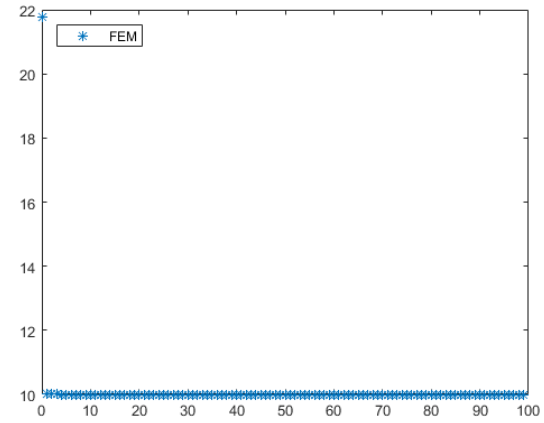

(a) Non-incremental $\eta = 1000$

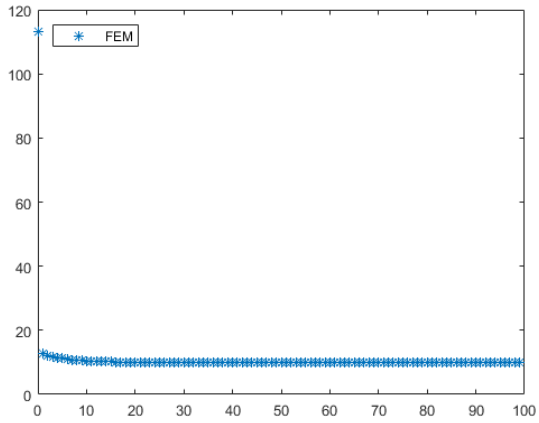

(b) Non-incremental $\eta = 10000$

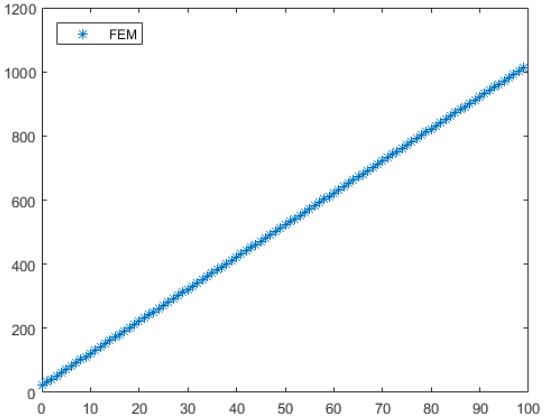

(c) Incremental $\eta = 1000$

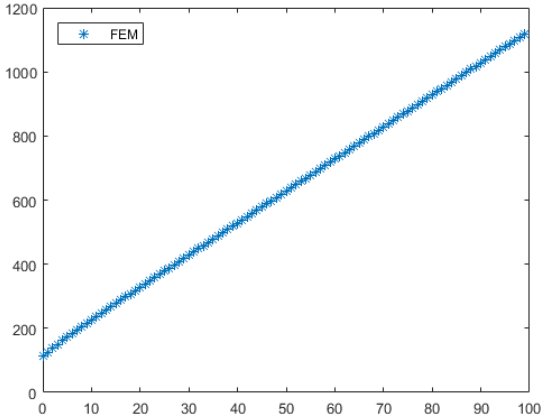

(d) Incremental $\eta = 10000$

Figure 5.2: Kelvin-Voigt with 1 unit displacement

For the Kelvin model the slope remain the same, but the peak values have been altered.

Secondly we have the Maxwell model, using the following parameters

- E = 1000
- $\eta = 10000$
- nt = 100
- displacement = 1
- $\varepsilon = \frac{displacement}{nt}$

- dt=1
- $\theta = 0.5$

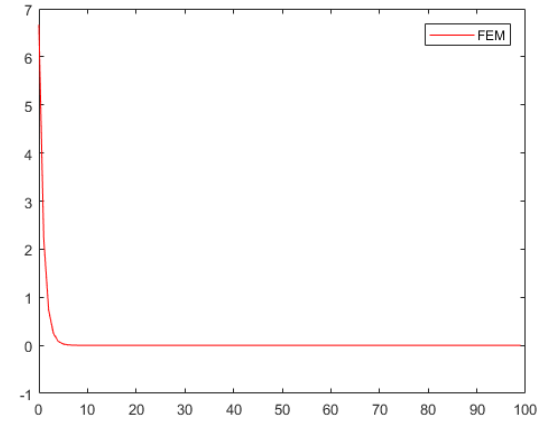

(a) Non-incremental $\eta = 1000$

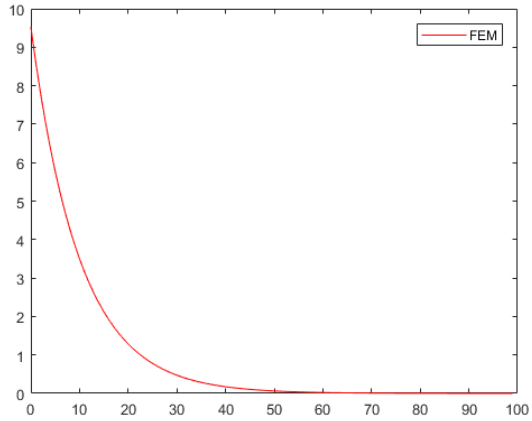

(b) Non-incremental $\eta = 10000$

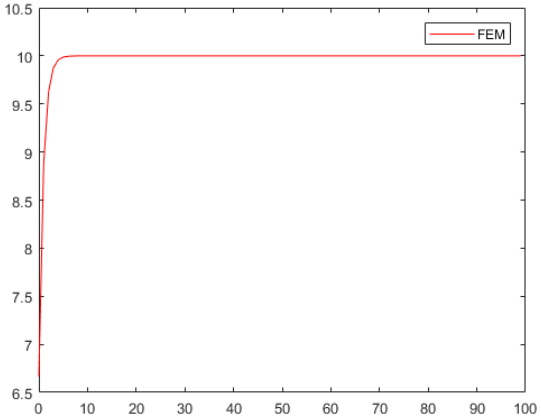

(c) Incremental $\eta = 1000$

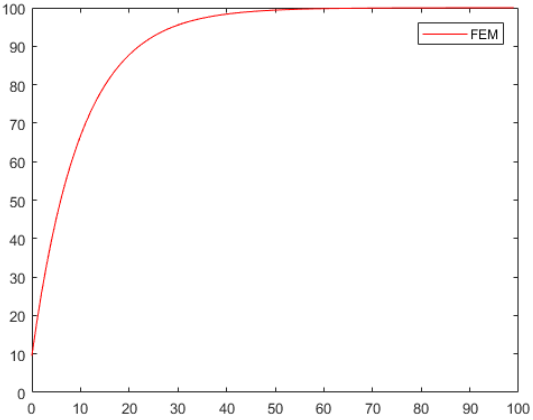

(d) Incremental $\eta = 10000$

Figure 5.3: Maxwell model with 1 unit displacement

Based on the plots, we can see how the value of η is affecting slope and peak values in the maxwell model. While for Kelvin it moves increases the stresses by a constant value for the incremental displacement, and is more or less not affecting the non-incremental displacement. This can also be seen from the equation $\sigma = E\varepsilon^e + \eta\dot{\varepsilon^v}$

Using the relations for the basic elements, the stress-strain relation for the Maxwell model is

$$\frac{\dot{\sigma}}{E} + \frac{\sigma}{\eta} = \dot{\varepsilon} \tag{74}$$

For this model total strain rate is the strain from the spring and the viscous dashpot, having equal stress in the two elements. The inelastic contribution stems from the viscous dashpot. From the equation above we see if $\dot{\varepsilon} = 0$(constant strain), the stress rate is proportional to the stress and decreasing in magnitude, we have stress relaxation. For constant stress, that is $\dot{\sigma} = 0$, the strain rate can be seen to be constant, thus implying a linear increase in strain with time, this is called creep.

The slope of the stress curve (σ_{xx}) produced with the Maxwell model is determined by the characteristic time($\tau_c = \frac{\eta}{E}$). By changing the characteristic time we expect different response. In the analysis there will only be done changes to the viscosity(η). First of all we are mainly interested in the behaviour and the trends of the results that can be seen. Changing the value of the modulus of elasticity(E) will change amplitudes in the stresses which again causes a change in the slope. However, it is easier to observe the behaviour when the stresses are not changed because of the modulus of elasticity as this would add one more thing to consider when comparing results. Secondly there have already been done tests to approximate the value of E.

The deformation power per unit volume of the Maxwell model is

$$\omega_d = \sigma\dot{\varepsilon} = \sigma\dot{\varepsilon}^e + \sigma\dot{\varepsilon}^i \tag{75}$$

Elastic power is therefore given as $\sigma\dot{\varepsilon}^e$, which is the energy being stored in the spring. While $D_i = \sigma\dot{\varepsilon}^i = \eta\dot{\varepsilon}^i\dot{\varepsilon}^i \geq 0$ is the inelastic dissipation of heat from the dashpot. This implies that the dashpot will always move in the direction of the applied stress. Non-negative dissipation is a requirement of the 2^{nd} law of thermodynamics

5.2 Analysis done on CNS

There have been run tests with several displacement fields, both viscoelastic models, with several material parameters. As the results are interpreted it is possible to narrow it down to do more in depth-analysis regarding the interesting inputs and parameters. Therefore I will not present the whole amount of results, I will rather in this section highlight areas of interest and results worth discussing.

The time discretization (dt) is put equal to 1. The relaxation time is varying from 1 second to 10 seconds. The modulus of elasticity (E) is kept equal to 1000Pa, while the two viscosity constants used (η) are $1000\frac{kg}{sm}$ and $10000\frac{kg}{sm}$

- E = 1000 MPa
- $\eta = 1000$ Pa·s
- dt=1 s
- $\theta = 0.5$
- $\nu = 0.3$

The units for distance measurements of the CNS is given in micrometers. Results obtained of the stresses are given in Pascal, and strains are without units. The embryo will often be in the area of 500μm. The CNS is clearly shorter than this, and as seen from the data the length is just a little more than 300μm.

For post-processing I will consider plots generated by matlab containing stresses, strains and position over time. Also I will use Paraview, which allows me to post-process VTK files generated from the analysis.

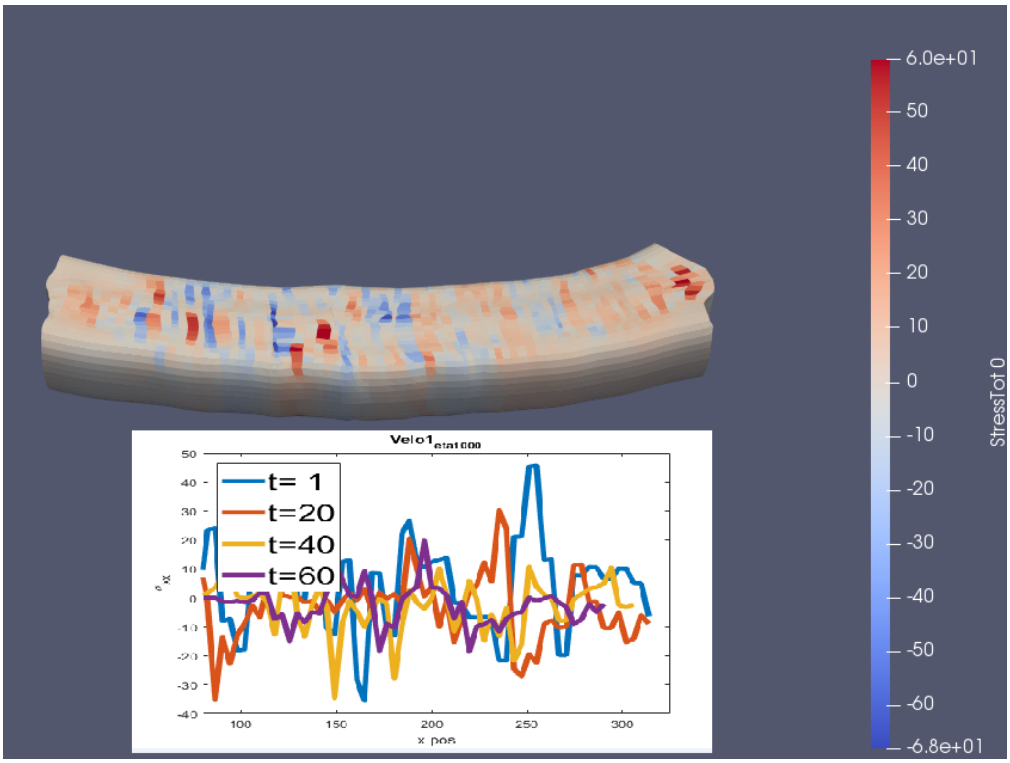

Figure 5.4: Maxwell stresses, with velocity1 and $\eta = 1000$ at time t=40

The stresses plotted can be seen to align with the stresses in paraview. Note that for every

cross section of the embryo through the A-P axis, there is done an average of the stresses which results in the stress plot produced by matlab. Every velocity field consist of 248 time steps.

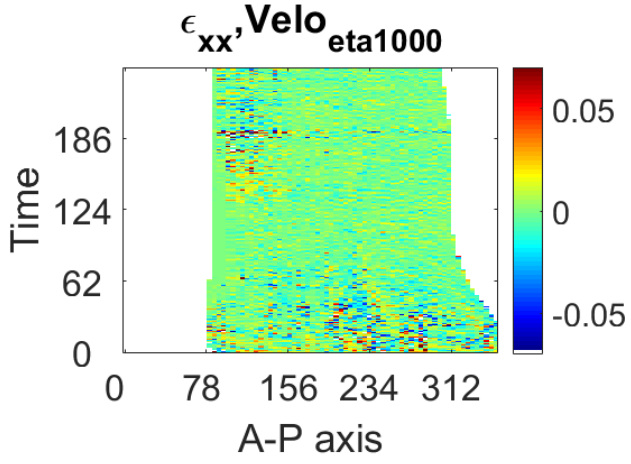

(a) Strains

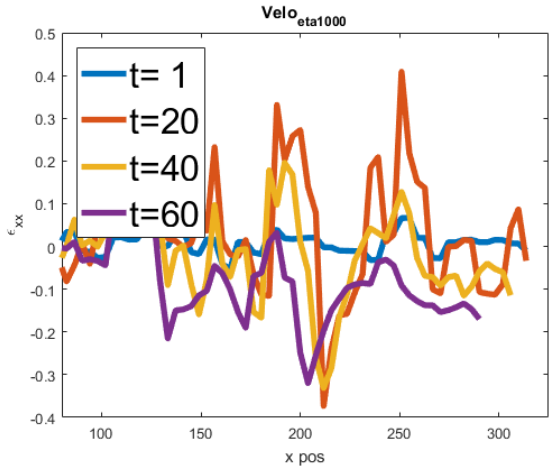

(b) Position & strains

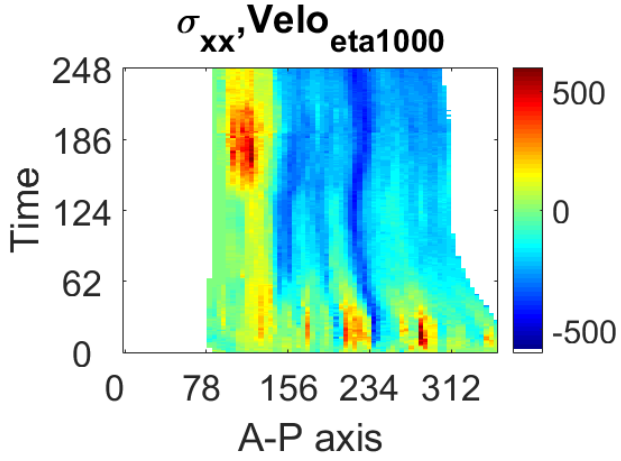

(c) Stresses

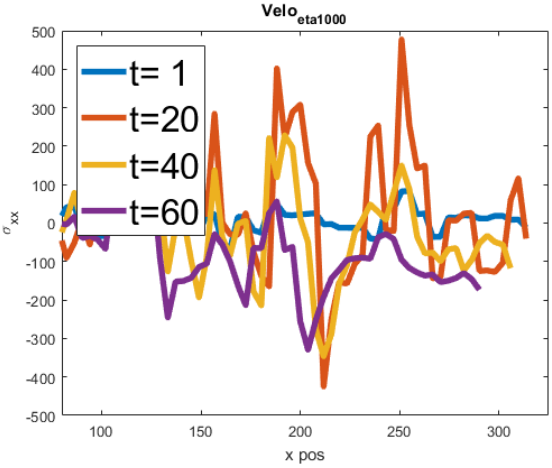

(d) Position & stresses

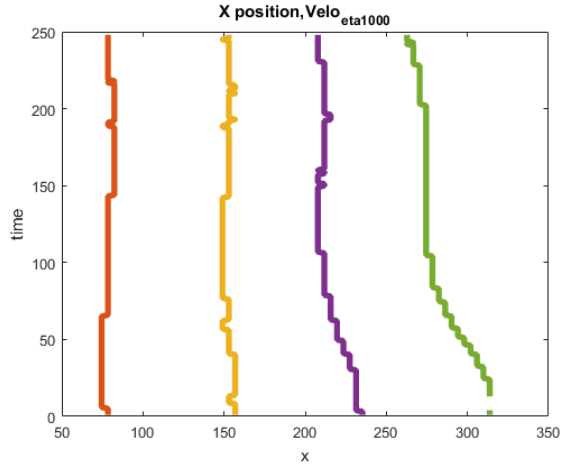

(e) X position

Figure 5.5: Kelvin model with velocity field 1 & $\eta = 1000$

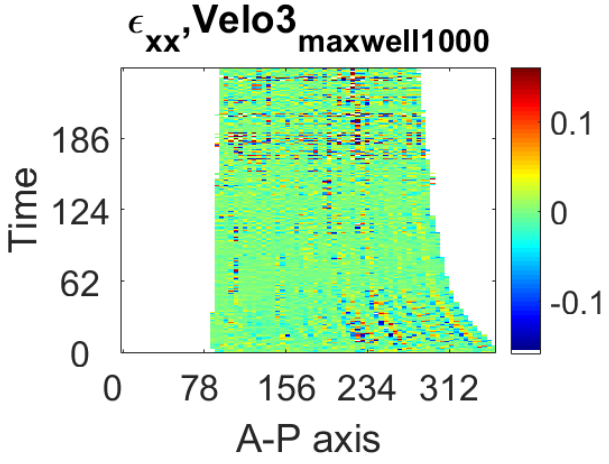

(a) Strains

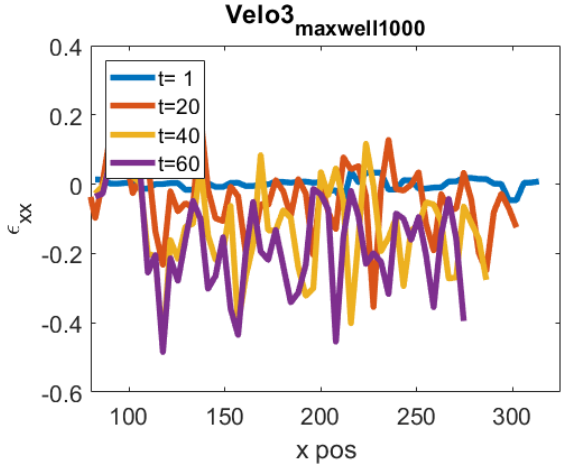

(b) Position & strains

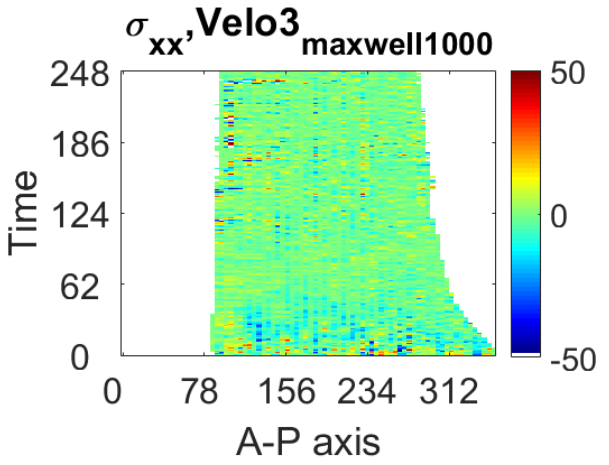

(c) Stresses

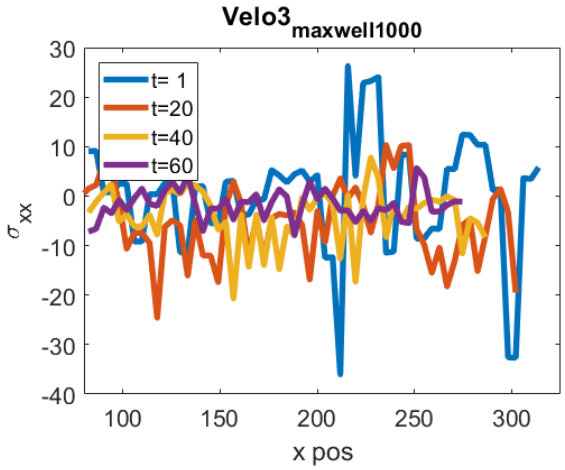

(d) Position & stresses

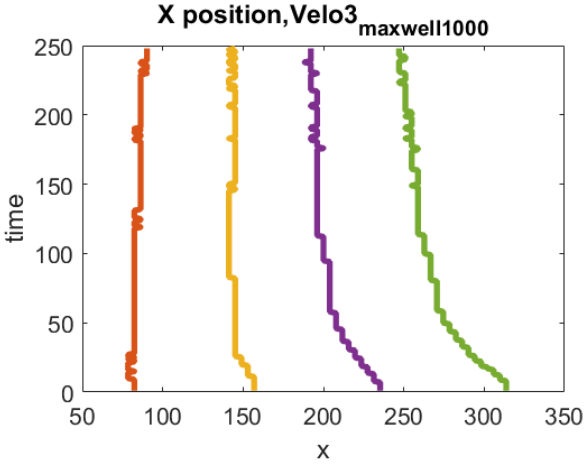

(e) X position

Figure 5.6: Maxwell model with velocity field 3 & $\eta = 1000$

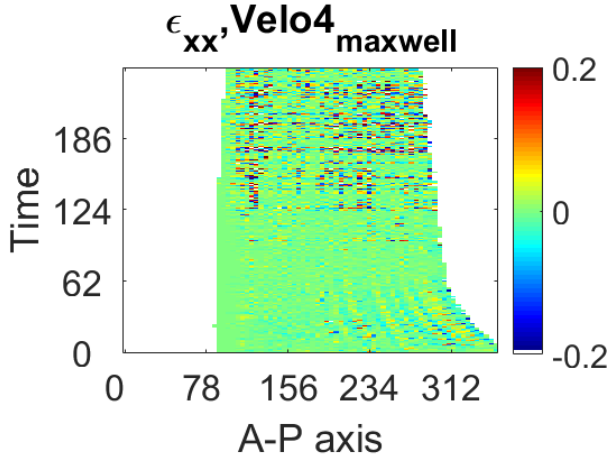

(a) Strains

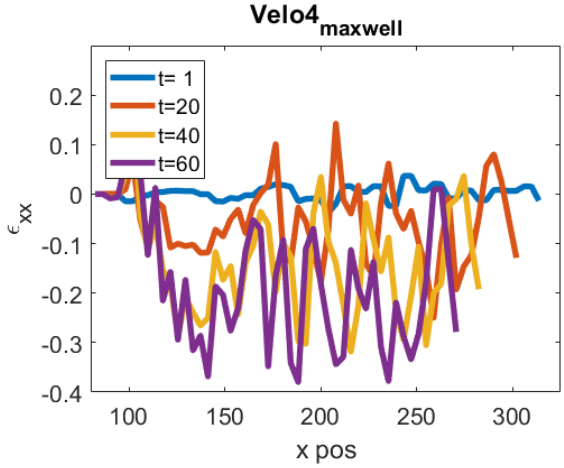

(b) Position & strains

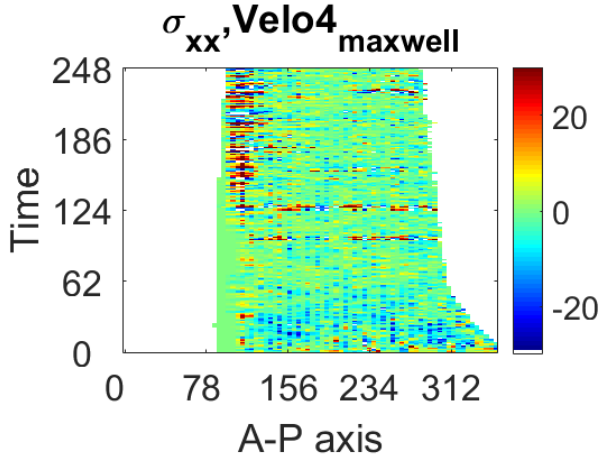

(c) Stresses

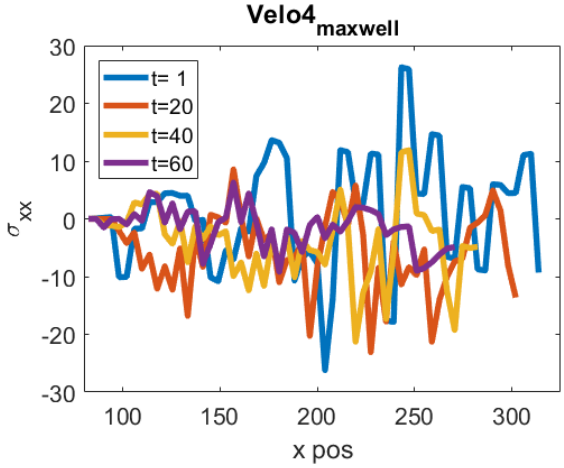

(d) Position & stresses

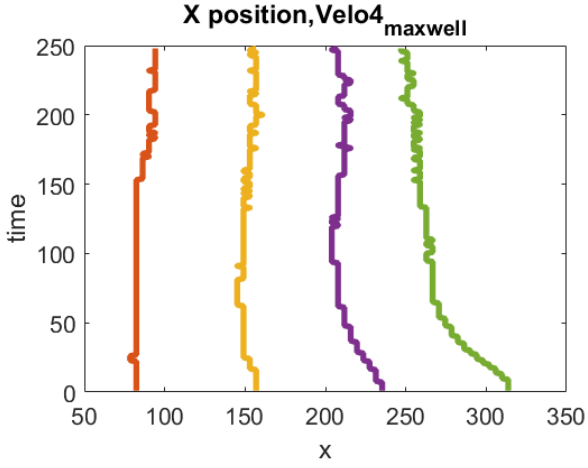

(e) X position

Figure 5.7: Maxwell model with velocity field 4 & $\eta = 1000$

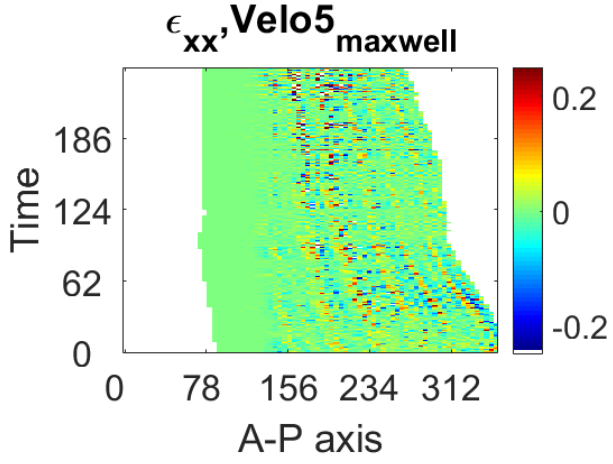

(a) Strains

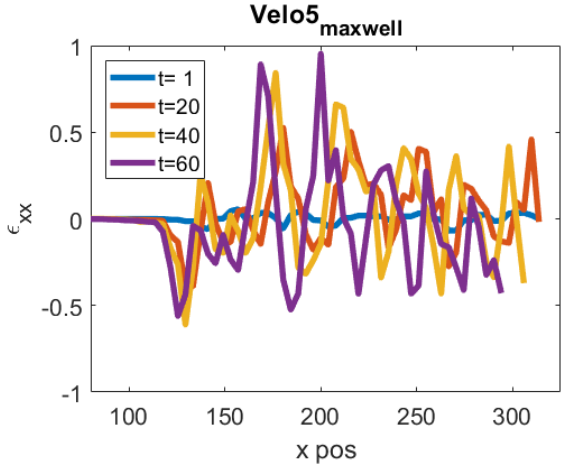

(b) Position & strains

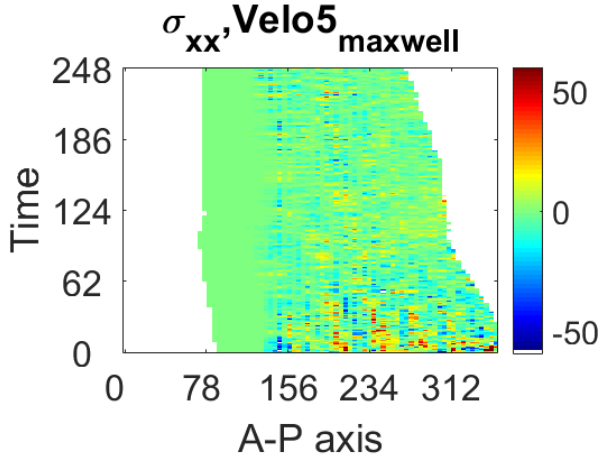

(c) Stresses

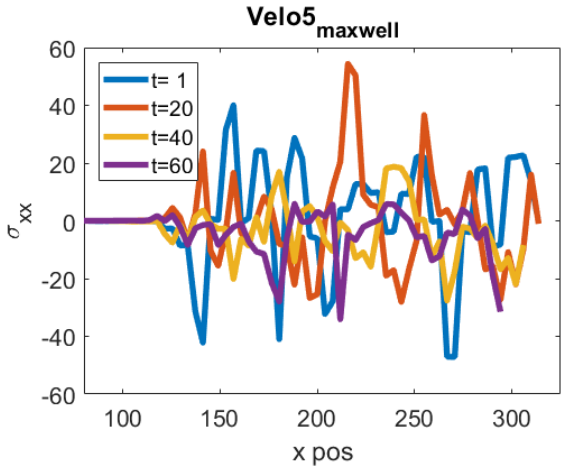

(d) Position & stresses

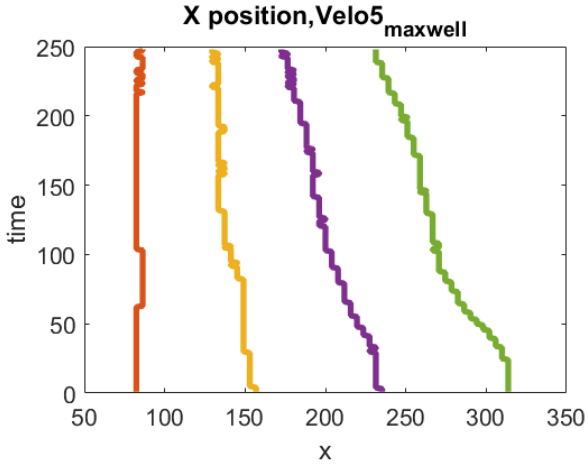

(e) X position

Figure 5.8: Maxwell model with velocity field 5 & $\eta = 1000$

The figures above show the plots generated by the matlab code and allows us to post-process.

It is possible to scale the colormap in order to give a good visualization of how the stresses and strains are developing in the embryo. A change of scales has been done in most plots in order to obtain a useful figure. Also all the mat.files have been saved and added as attachments. This is making it possible to load the files again and use matlab functions to reproduce the figures, and also to change variables to highlight certain areas of the simulation done. In addition, all the outputVTK files have been stored and attached. These files contain stresses, strains and displacements of the embryo. As shown earlier these files can be opened and visualized in visualization programs such as paraview.

For both the Maxwell and the Kelvin model it is evident that by increasing the viscosity, we also increase the stresses. For the Maxwell model the strains seem to respond less for the change in viscosity. While for the Maxwell there can be seen larger strains with higher viscosity, note that the strains and stresses are proportional.

By comparing the deformations in velocity 1,3,4 and 5 it is quickly visible how the first velocity field is an outlier from the others as its deformation is far from as significant in the AP-axis. As the magnitude of the stresses from velocity field 1 is also not comparable with the rest I chose to disregard this field.

(a) Velocity field 1

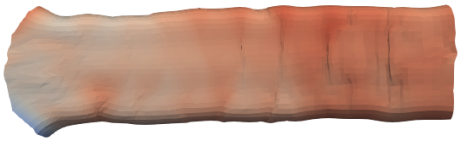

(b) Velocity field 3

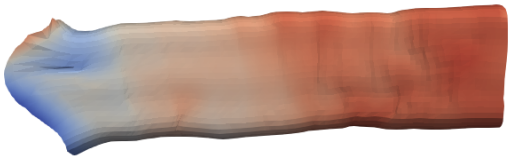

(c) Velocity field 4

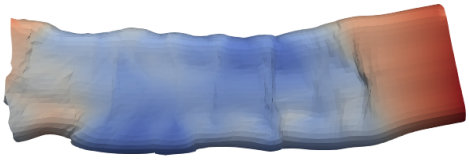

(d) Velocity field 5

Figure 5.9: Displacement in y-direction at time step 80

Above we can see how the embryo is deformed at t=80. The intensity of the colors symbolise the intensity of the displacements in the y-direction. Where x-direction is the AP-axis.

In the three remaining fields the magnitude of displacement in the AP axis is more or less comparable, with velo3 being in the middle. It is visible that both velo4 and velo5 produce a larger curvature perpendicular to the AP-axis, while velo3 exhibit a straighter contraction without much movement in any other direction.

The displacement field of velo5 is curving relatively much compared to velo1 and velo3. This kind of curving might be produced by rigid body motion which again may alter the results.

When considering the displacements it is important to check for several values, as the displacement field may vary slightly for the same velocity field. Different material parameters will alter the displacements, also some scenarios can produce local numerical errors. Therefore it is important to consider the displacement for more than one situation for each velocity

field.

For Kelvin we can see how the stresses initially have large positive values, while later when the larva has contracted already the pattern is still visible, but now with negative stresses except from on the left hand side, which may be caused by being close to the boundary. Strains and stresses are clearly proportional with the same segments.

We may observe that for this viscoelastic model the stresses do not decrease in the same pace for t=60 as we could see in the maxwell model. Instead the stresses in the Kelvin model is clearly following a proportional value of the strains. This happens regardless of the viscosity constant and the velocity field.

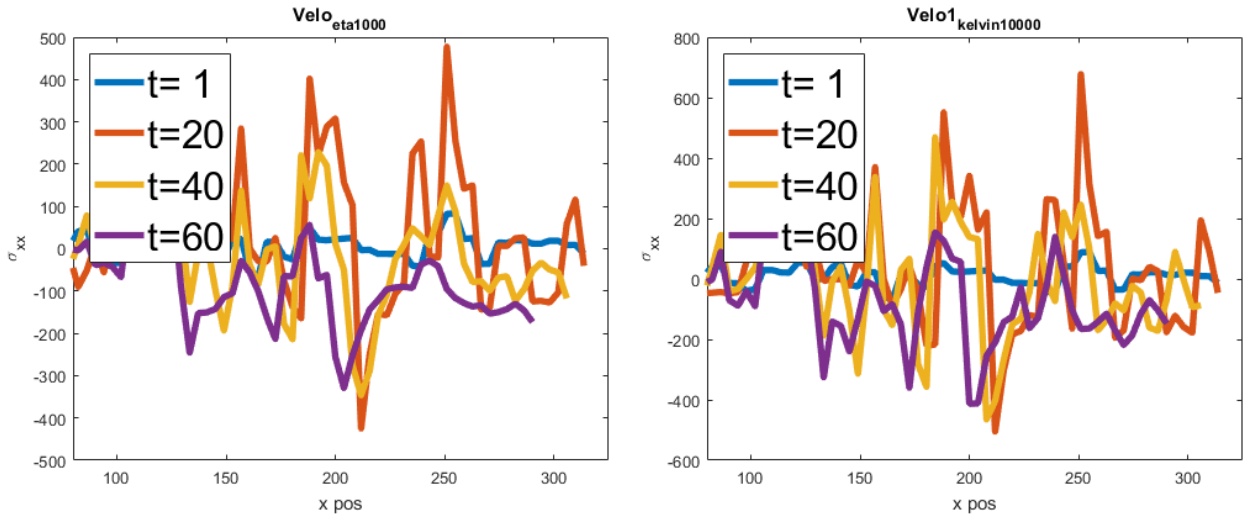

(a) $\eta = 1000$ **(b)** $\eta = 10000$

Figure 5.10: Kelvin stresses with velocity 1

The same goes for the strains in Kelvin model

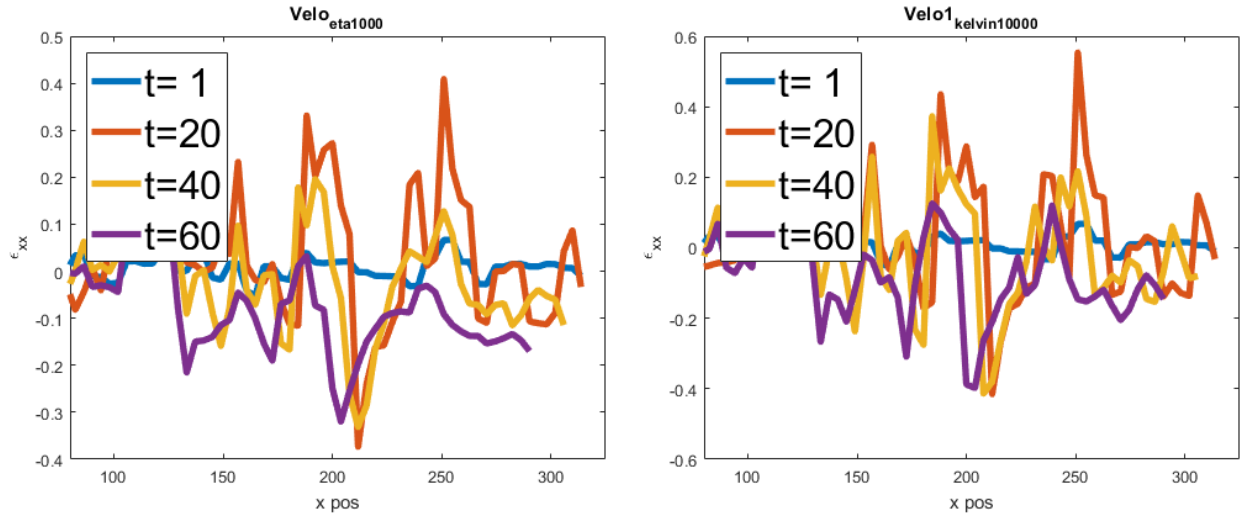

(a) $\eta = 1000$ **(b)** $\eta = 10000$

Figure 5.11: Kelvin strains with velocity 1

The Kelvin shows non-physical behavior and allows accumulation of stresses. The Kelvin model, is accumulating stress because the spring is in parallel with the damper, the forces will always increase with strains as shown in figures (c) and (d) presented, in contrast to Maxwell where the damper can move without the spring and have time to relax. The strains in the embryo is happening over a large time period, with larger deformations. Thus the Kelvin model seems to be unsuitable. Note much larger stresses for the Kelvin model.

5.2.1 Post-processing

In general all simulations run shows the correlation between characteristic time and stresses. Increasing the viscosity will lead to an increase in stresses. As time passes by the developed stresses in the larva is decreasing, as suported by the figures above. It can be seen from how the blue lines have larger peaks and average values than the purple lines. In addition, maybe even more clear it becomes by studying the colormap showing the stresses from start to end.

In some cases there is a obvious stress concentration on the left hand side of the colormap. These I will not consider as they seem nonphysical and are close to boundaries which may cause them.

Note that the purple and last line only consider time interval 60, which is still is an relatively early stage of the development. However, the trend is that from this point and out the oscillations are decreasing very slowly and so are the stress peaks.

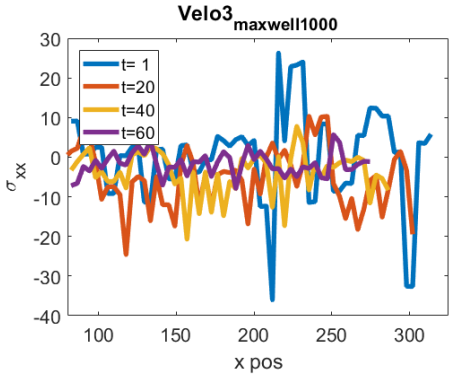

Figure 5.12: Position & stresses for velocity 3 and $\eta = 1000$

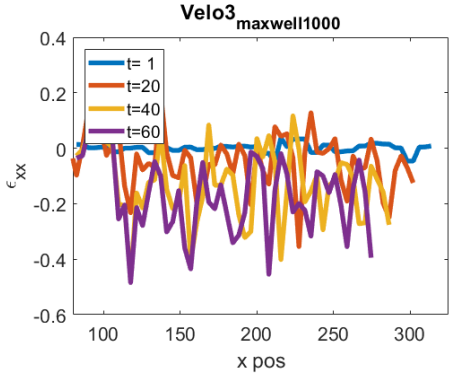

Figure 5.13: Position & strains for velocity 1 and $\eta = 1000$

We may see from the figures (b) that during the development, the final x-position is moving to the left, we are seeing the contraction in the development. So it is also possible to find the velocity of the development by considering the displacement between timesteps.

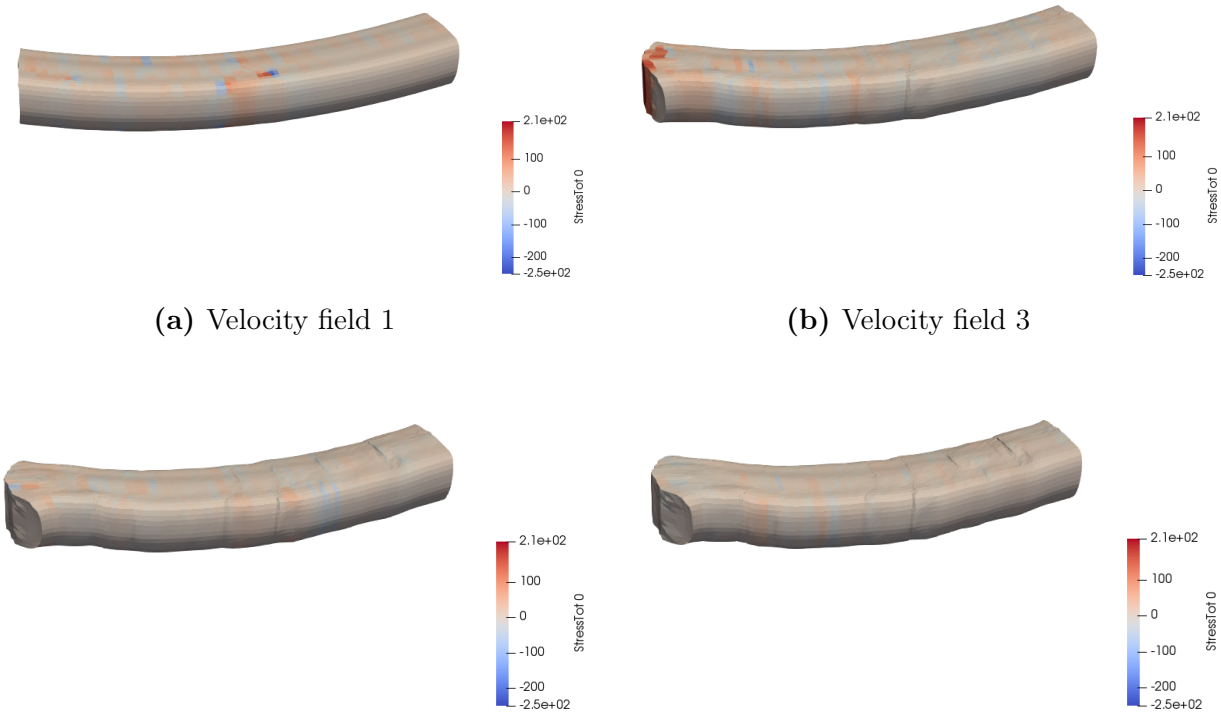

(a) Velocity field 1

(b) Velocity field 3

(c) Velocity field 4

(d) Velocity field 5

Figure 5.14: Stresses in AP-direction for velocity 3 Maxwell model

Up to this point we have considered stresses and strain with respect to position up to t=60, up to this point as seen from the colormap is also where the main deformation is happening. Let us now consider time intervals from t=60. This I will do for different values of characteristic time with the maxwell model on the third velocity field.

To investigate further I will now also present the same case, however, this time I will consider some other values of η, 5000 and 10 000 respectively.

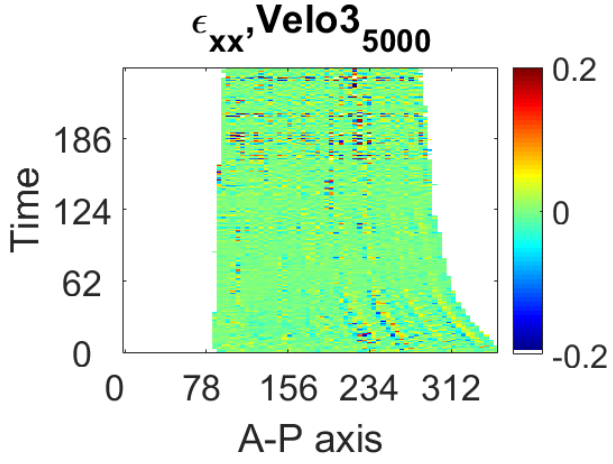

(a) Strains

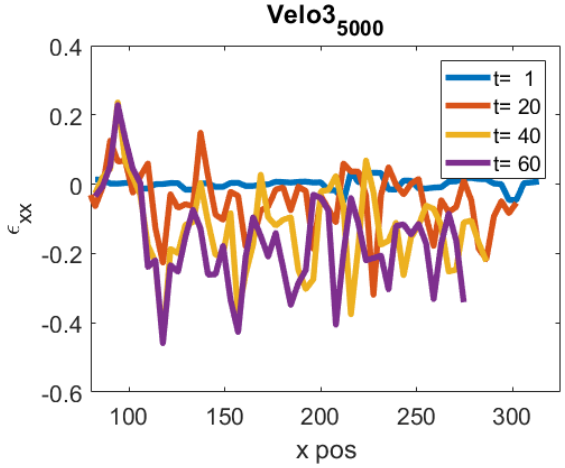

(b) Position & strains

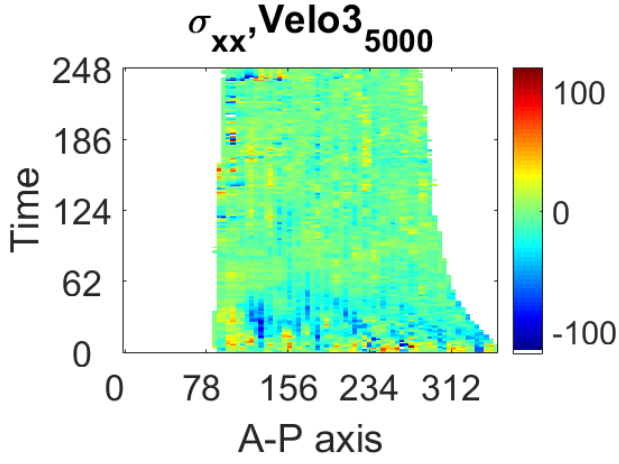

(c) Stresses

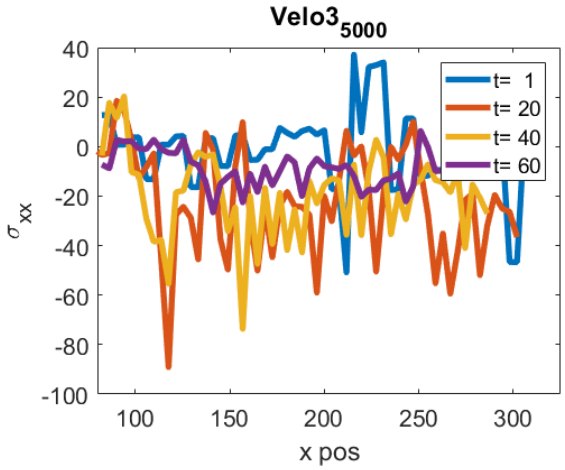

(d) Position & stresses

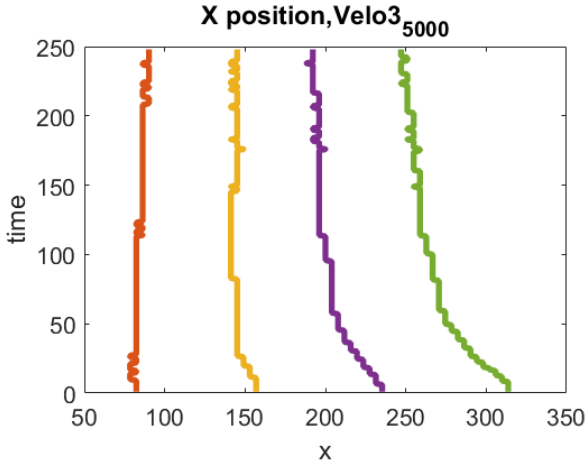

(e) X position

Figure 5.15: Maxwell velocity field 3 & $\eta = 5000$

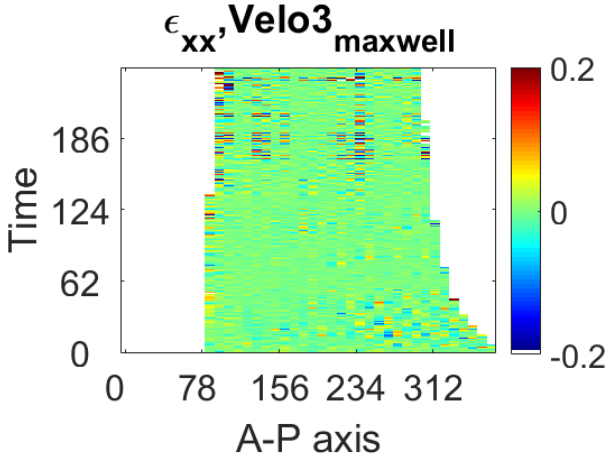

(a) Strains

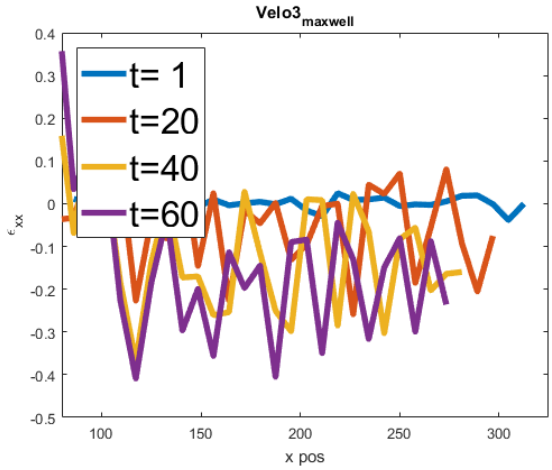

(b) Position & strains

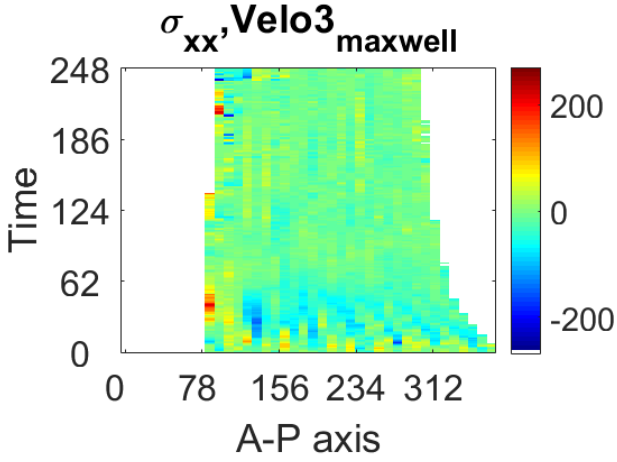

(c) Stresses

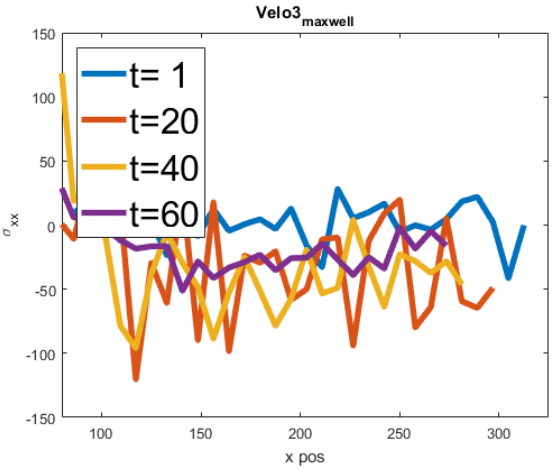

(d) Position & stresses

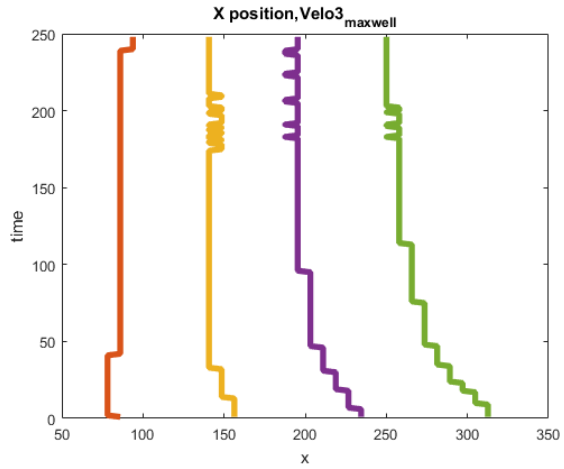

(e) X position

Figure 5.16: Maxwell velocity field 3 & $\eta = 10000$

Further I have for simulations plotted the values of the strains and stresses with respect to the position for time intervals after t=60.

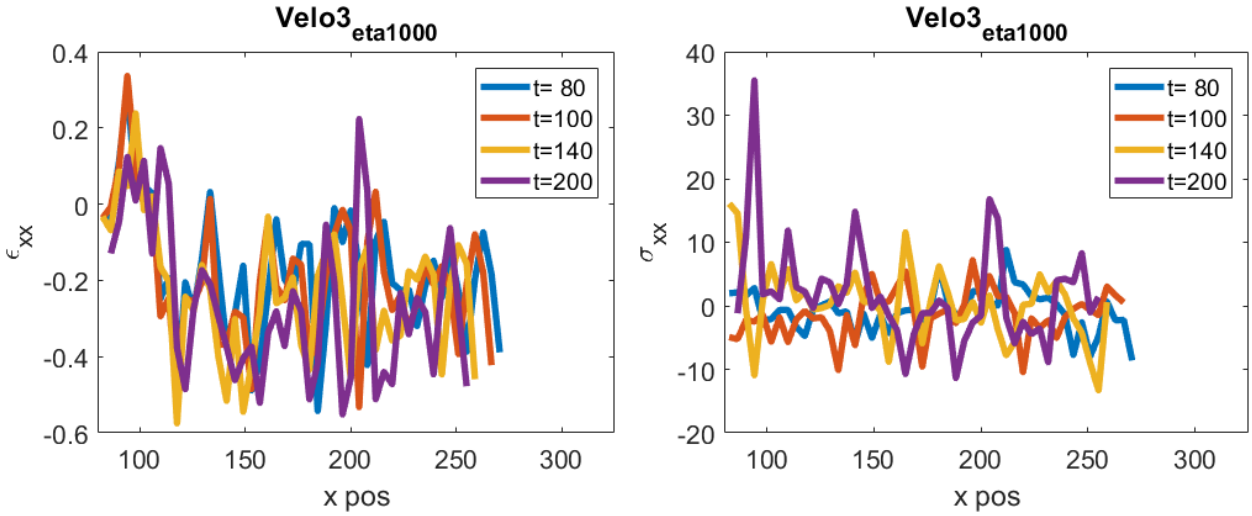

(a) Strains **(b)** Stresses

Figure 5.17: Maxwell model with velocity 3 and $\eta = 1000$

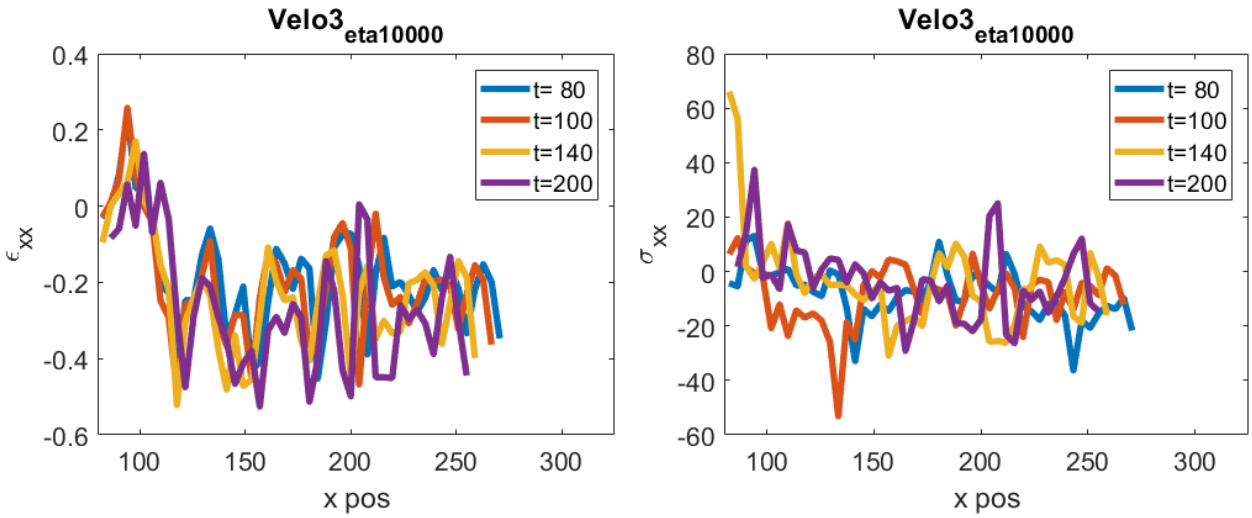

(a) Strains **(b)** Stresses

Figure 5.18: Maxwell model with velocity 3 and $\eta = 10000$

Observe that the strains are are not experiencing close to as much decay as the stresses are over time. This is clear from the figures above, and even more clear when you consider figure

7.6b and 7.6d containing timesteps from 1 to 60. Increasing the viscosity will lead to an increase in stresses. As time passes by the developed stresses in the larva is decreasing.

From the position plots, it is clearly that there is a segmentation in the embryo, for instance we can see this from the oscillations of stresses and strains along the AP-axis of the larva. Actually, we are also able to track the segments based on the colormap, as displaced lines over time that are experiencing peak values in both stresses and strains.

Velocity three produce a clear pattern in the strains that is repeated for both the Maxwell model and the Kelvin model for different values of η. We see how for a given position in different time interval there is a contraction, this shows how parts of the embryo have segmented behavior.

Note also that the final position on the x-axis is shortened by time, showing how the embryo is contracting, eventually becoming shorter and shorter.

It seems like the embryo initially exhibit both compression and tension due to positive and negative stresses. In general the larva will contract. While both tension and compression is decreasing slowly over time, the body contracts and it seems like the compression is decaying slower.

6 Conclusion

As a viscoelastic model, it is shown that the Maxwell model with the spring and dashpot in series is modelling embryo development in a much better way than the Kelvin model can. The model with varying material parameters have presented a set of plausible stresses developed in embryo development. Viscosity changes have for this scenario a large impact on results obtained for the Maxwell model.

There is an obvious oscillatory characteristic behavior in the embryo development. We are able to how the peak values of both stresses and strains in the larva during development is alternating between maximum and minimum values throughout the whole process, however with a tendency of decay. In addition it is shown how the larva seems to be consisting of different parts or segments along the AP-axis. We can from the oscillations through time see how the parts can be tracked along the displacement, but with a clear velocity in contracting direction.
Initially in the beginning of deformation, a pattern alternating between compression and tension is obvious, once again highlighting the pattern of segmentation. The position of tension and compression can be tracked along time by studying the colormaps over time.

As the velocity fields studied give varying results, we can see that accuracy is highly dependent on accuracy of the measured experimental data.

If one study the deformation of the CNS over time we can see a that deformation is decaying over time, but in addition it is possible to spot a trend of three phases. An initial contraction phase is evident, while there is a trend of a decay or a pause phase, before finally there is a new contraction phase.

-

7 References

1. F. Irgens. Continuum Mechanics. Springer, (2008).
2. Material Mechanics, Odd Sture Hopperstad and Tore Børvik, (2017)
3. Drosophila melanogaster neurobiology, neuropharmacology, and how the fly can inform central nervous system drug discovery, Charles D. Nichols
4. How to map the circuits that define us, Kerri Smith, (2017)